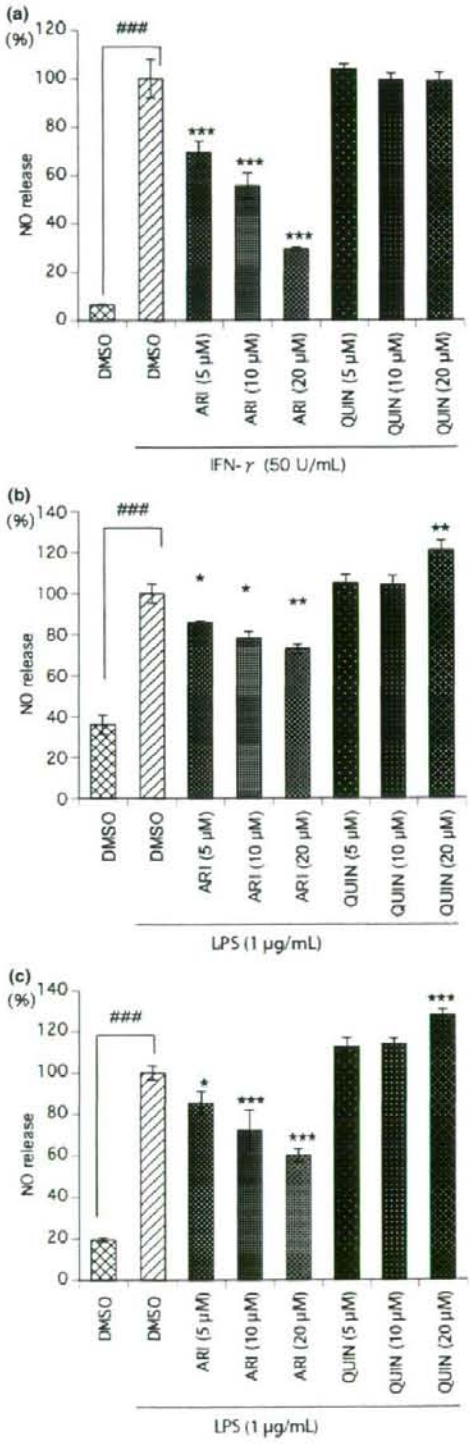

Fig. 2 The effect of aripiprazole on NO release by activated microglia (a) & (b). The 6-3 microglial cells were pre-treated with DMSO (0.1%), aripiprazole (5, 10 and 20 μM) or quinpirole (5, 10 and 20 μM) for 12 h, then the cells were treated with each drug and IFN-γ (50 U/mL) (a) or LPS (1 μg/mL) (b) for 48 h. NO release were determined using the Griess assay. The results were expressed as the percentage values taking the IFN-γ or LPS + DMSO treatment group as 100%. All Data are represented as the means (SEM) of three independent experiments ($n = 15$). ###$p < 0.001$ in comparison to the control DMSO treatment group. *$p < 0.05$; **$p < 0.01$; ***$p < 0.001$ in comparison to the IFN-γ or LPS + DMSO treatment group. (c) Rat primary microglial cells were pre-treated with DMSO (0.1%), aripiprazole (5, 10 and 20 μM) or quinpirole (5, 10 and 20 μM) for 12 h, then the cells were treated with each drug and LPS (1 μg/mL) for 48 h. NO release were determined using the Griess assay. The results were expressed as the percentage values taking the LPS + DMSO treatment group as 100%. All Data are represented as the means (SEM) of three independent experiments ($n = 15$). ###$p < 0.001$ in comparison to the control DMSO treatment group. *$p < 0.05$; ***$p < 0.001$ in comparison to the LPS + DMSO treatment group.

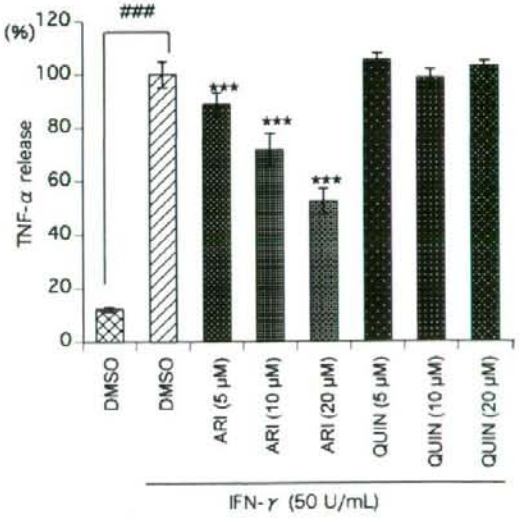

Fig. 3 The effect of aripiprazole on TNF-α release by IFN-γ-activated microglia. The 6-3 microglial cells were pre-treated with DMSO (0.1%), aripiprazole (5, 10 and 20 μM) or quinpirole (5, 10 and 20 μM) for 12 h, then the cells were treated with each drug and IFN-γ (50 U/mL) for 48 h. TNF-α release were determined using the ELISA, respectively. The results were expressed as the percentage values taking the IFN-γ + DMSO treatment group as 100%. All Data are represented as the means (SEM) of three independent experiments ($n = 15$). ###$p < 0.001$ in comparison to the control DMSO treatment group. ***$p < 0.001$ in comparison to the IFN-γ + DMSO treatment group.

of TNF-α (Fig. 3). Aripiprazole or quinpirole itself had no effect on releasing NO and TNF-α without IFN-γ treatment (data not shown).

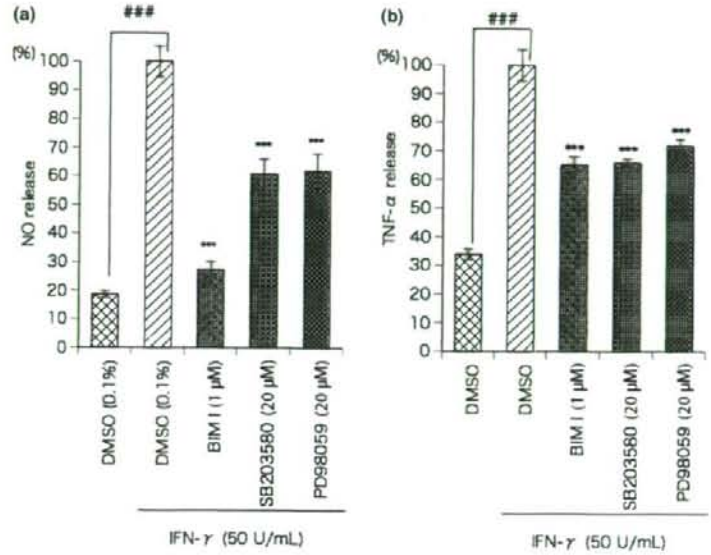

Fig. 4 The effect of inhibitors on NO and TNF-α release by IFN-γ-activated microglia. NO (a) and TNF-α (b) release were determined using the Griess assay and ELISA, respectively. The 6-3 microglial cells were pre-treated with 1 μM BIM I (PKC inhibitor), 20 μM SB203580 (p38 MAPK protein inhibitor) or 20 μM PD98059 (MAPK protein inhibitor, for ERK) for 1 h, then the cells were treated with each drug and IFN-γ (50 U/mL) for 24 h. The results were expressed as the percentage values taking the IFN-γ + DMSO treatment group as 100%. All Data are represented as the means (SEM) of three independent experiments ($n = 15$). ###$p < 0.001$ in comparison to the DMSO control group. ***$p < 0.001$ in comparison to the IFN-γ + DMSO treatment group.

The intracellular signaling mechanism in NO and TNF-α release from IFN-γ-activated microglia

The 6-3 murine microglial cells were pre-treated with 1 μM BIM I (PKC inhibitor), 20 μM SB203580 (p38 MAPK protein inhibitor) or 20 μM PD98059 (MAPK protein inhibitor, for ERK) for 1 h, then the cells were treated with each drug and IFN-γ (50 U/mL) for 24 h. BIM I, SB203580 and PD98059 significantly inhibited NO and TNF-α release from IFN-γ-activated microglia (Fig. 4a and b). In comparison to the positive controls (DMSO), the specific inhibition of PKC, p38 MAPK and ERK was observed to lead to a decrease in the NO release to 27.3 ± 2.84%, 60.6 ± 5.29% and 61.7 ± 6.14%, respectively, while the specific inhibition of PKC, p38 MAPK and ERK was found to lead to a decrease in TNF-α release to 65.3 ± 2.72%, 66.0 ± 1.48% and 71.9 ± 2.25%, respectively. Each inhibitor treatment did not have any effect on the cell viability (data not shown). These results suggest that the PKC, p38 MAPK and ERK pathways all play key roles in IFN-γ-induced activation of the 6-3 murine microglial cells.

Aripiprazole attenuates the mobilization of intracellular Ca^{2+} induced by IFN-γ-activated microglia

In human microglia, IFN-γ rapidly induces a progressive increase in $[Ca^{2+}]_i$ and IFN-γ acts solely through influx of Ca^{2+} (Franciosi *et al.* 2002) and $[Ca^{2+}]_i$ is very important for the regulation of microglial activation including the release of NO and cytokines (Hoffmann *et al.* 2003).

We measured the effect of 12 h treatment with quinpirole (10 μM) or aripiprazole (5 μM) on the mobilization of intracellular Ca^{2+} induced by IFN-γ application in the 6-3 cells. As shown in Fig. 5(a), IFN-γ (50 U/mL) rapidly increased $[Ca^{2+}]_i$ in the 6-3 cells (pretreated with 0.025% DMSO for 12 h; $n = 10$ cells). Once the intracellular Ca^{2+} rose, it gradually increased without attenuation. The increase in intracellular Ca^{2+} was sustained > 40 min after the washout of IFN-γ until the end of recording. Therefore, IFN-γ induced sustained intracellular Ca^{2+} elevation in the murine microglia as previously shown in human microglia (Franciosi *et al.* 2002).

In the 6-3 cells pre-treated with quinpirole (10 μM) or aripiprazole (5 μM) for 12 h, IFN-γ (50 U/mL) also induced sustained intracellular Ca^{2+} elevation (Fig. 5b and c; $n = 23$ for quinpirole and $n = 28$ for aripiprazole). However, the amplitude of $[Ca^{2+}]_i$ increase induced by IFN-γ was very different between the cells pre-treated with quinpirole or aripiprazole. The treatment of quinpirole (10 μM for 12 h) did not affect the amplitude of increase in $[Ca^{2+}]_i$ induced by IFN-γ in the cells (230.4 ± 26.8 nM in DMSO vs. 219.1 ± 34.8 nM in quinpirole; $p = 0.76$). In contrast, pre-treatment with aripiprazole (5 μM for 12 h) significantly reduced the amplitude of increase in $[Ca^{2+}]_i$ at 10 min after a 5-min treatment of IFN-γ (DMSO vs. 80.0 ± 7.50 nM in aripiprazole; $p < 0.001$) (Fig. 5d).

The 6-3 cells were pre-treated with or without the membrane-permeable intracellular Ca^{2+} chelator, BAPTA-AM (5 μM and 20 μM), then the cells were treated with IFN-γ (50 U/mL) for 24 h. BAPTA significantly decreased NO release from IFN-γ-activated microglia (Fig. 5e) without cytotoxicity (MTT data not shown), which was the same as the previously reported findings of Hoffmann *et al.* (Hoffmann *et al.* 2003).

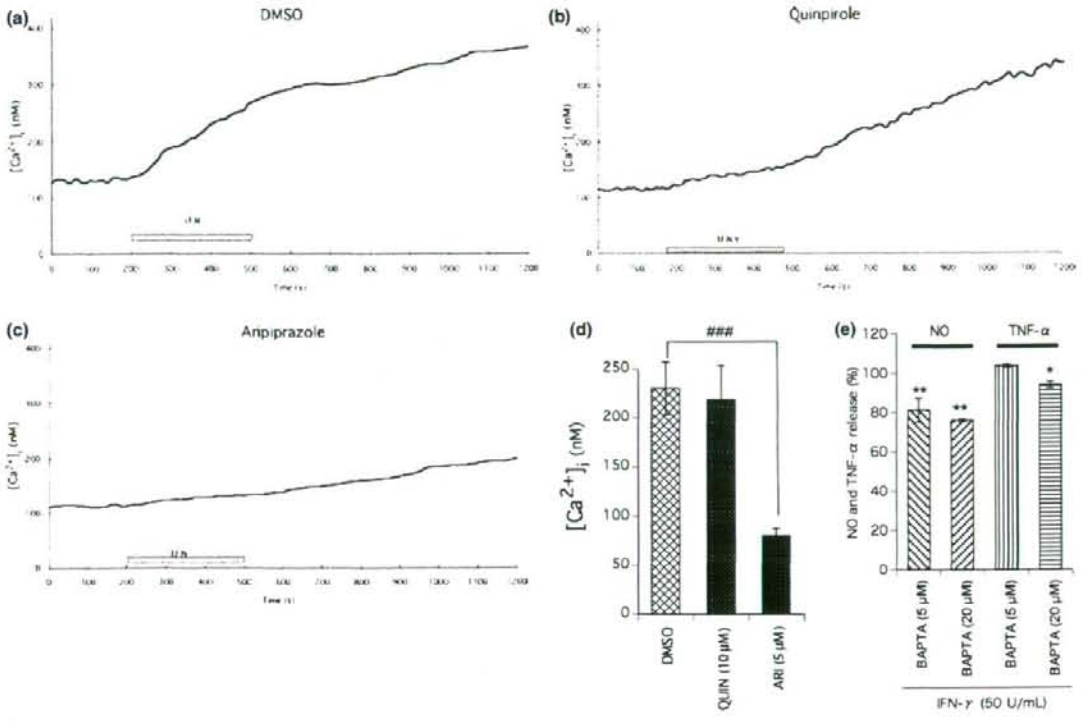

Fig. 5 The mobilization of intracellular Ca^{2+} induced by IFN-γ-activated microglia Sustained elevation of intracellular Ca^{2+} induced by IFN-γ application in the murine 6-3 microglial cells. Microglial cells were pre-treated with DMSO (0.025%) (a), quinpirole (10 μM) (b) or aripiprazole (5 μM) (c) for 12 h and then activated by IFN-γ (50 U/mL) for 5 min. Each panel shows the average trace of representative 15 traces of $[Ca^{2+}]_i$ in each condition. The increase in the $[Ca^{2+}]_i$ in response to IFN-γ application was calculated as the difference between basal $[Ca^{2+}]_i$ and values obtained at 10 min after a 5-min treatment of IFN-γ (d). Data are represented as the means (SEM) of each experiment. ###$p < 0.001$ in comparison to the DMSO treatment group. The 6-3 microglial cells were pre-treated with BAPTA-AM (5 μM and 20 μM), then the cells were treated with IFN-γ (50 U/mL) for 24 h (e). The results were expressed as the percentage values taking the IFN-γ treatment group as 100%. Data are represented as the means (SEM) of three independent experiments ($n = 15$). *$p < 0.05$; **$p < 0.01$ in comparison to the IFN-γ treatment group.

These results suggest that 12-h treatment of aripiprazole attenuates the mobilization of intracellular Ca^{2+} induced by IFN-γ application in the 6-3 murine microglial cells. The similar results were observed in rat primary microglial cells (data not shown).

Cell viability

The 6-3 cells were treated with DMSO (0.1%), aripiprazole (5, 10 and 20 μM) or quinpirole (5, 10 and 20 μM) for 60 h, or the 6-3 cells were pre-treated with DMSO (0.1%), aripiprazole (5, 10 and 20 μM) or quinpirole (5, 10 and 20 μM) for 12 h and then the cells were treated with each drug and IFN-γ (50 U/mL) for 48 h. Aripiprazole and quinpirole showed no significant microglial cytotoxicity at a concentration of less or equal 10 μM (Fig. 6a and b). IFN-γ treatment alone did not have any effect on the cell viability as previously demonstrated (Kato *et al.* 2007). The PC12 cells were treated with DMSO (0.1%) or aripiprazole (5, 10 and 20 μM) for 60 h. Aripiprazole showed no significant neuronal cytotoxicity under a concentration of 20 μM (Fig. 6c).

Discussion

In the present study, the generation of NO and TNF-α from IFN-γ-activated microglia was significantly inhibited by aripiprazole. In addition, aripiprazole suppressed the IFN-γ-induced elevation of $[Ca^{2+}]_i$ in microglia. Aripiprazole was not toxic either to microglial cells or neuronal cells at the concentrations where the effects described above were observed. The generation of NO and TNF-α from IFN-γ-activated microglia was significantly inhibited by specific inhibitors of PKC, p38 MAPK and ERK, respectively. In addition, aripiprazole significantly inhibited NO release from both LPS-activated 6-3 microglia and LPS-activated rat

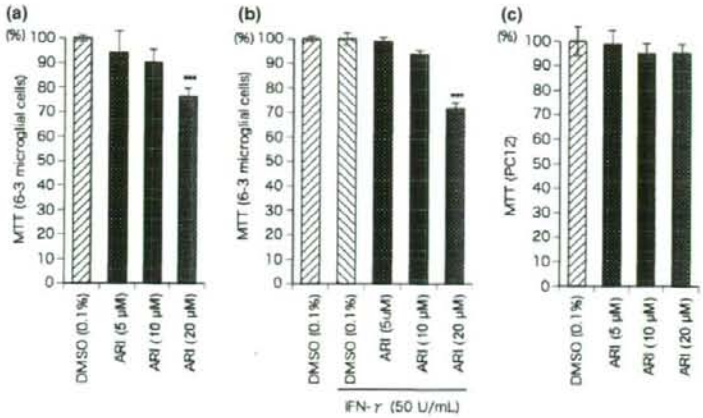

Fig. 6 Cell viability. Cell viability was determined by colorimetric measurements of the reduction product of 3-[4,5-dimethylthiazol-2-yl]-2,5-diphenyltetra-zolium bromide (MTT). The 6-3 microglial cells were treated with DMSO (0.1%), aripiprazole (5, 10 and 20 μM) or quinpirole (5, 10 and 20 μM) for 60 h (a), or the 6-3 microglial cells were pre-treated with DMSO (0.1%), aripiprazole (5, 10 and 20 μM) or quinpirole (5, 10 and 20 μM) for 12 h and then the cells were treated with each drug and IFN-γ (50 U/mL) for 48 h (b). The results were expressed as percentage values while taking the DMSO treatment group as 100% (a) or the DMSO plus IFN-γ treatment group as 100% (b), respectively. The PC12 cells were treated with DMSO (0.1%) or aripiprazole (5, 10 and 20 μM) for 60 h (c). The results were expressed as percentage values while taking the DMSO treatment group as 100% (c). All Data are represented as the means (SEM) of three independent experiments ($n = 15$), respectively. $^{***}p < 0.001$ in comparison to the DMSO treatment group.

primary microglia while quinpirole did not inhibit the NO release by LPS-activated 6-3 microglia or LPS-activated rat primary microglia.

Interferon-γ, which is one of the typical activators of microglia along with lipopolysaccharide (LPS), has recently been reported to induce Ca^{2+} influx in human microglia (Franciosi *et al.* 2002). We also observed that IFN-γ induced sustained $[Ca^{2+}]_i$ elevation in murine microglia. Hoffmann *et al.* demonstrated that the treatment of BAPTA can inhibit the release of NO and cytokines from LPS-activated microglia while ionomycin, an ionophore elevating Ca^{2+}, has no effect on the release of NO or cytokines from LPS-activated microglia. They thus indicated that an increased amount of $[Ca^{2+}]_i$ is required, but by itself is not sufficient, for the release of NO and certain cytokines from activated microglia (Hoffmann *et al.* 2003). We observed that the pre-treatment of aripiprazole attenuated the mobilization of intracellular Ca^{2+} induced by IFN-γ in murine microglia. Intracellular Ca^{2+} is one of the endogenous activators of PKC. Phorbol 12-myristate- 13-acetate, an activator of PKC, induces the activation of microglia (Nikodemova *et al.* 2006). In microglia, PKC has been reported to be an important initiator of the MAPK signaling pathway in the CNS. The activation of PKC affects MAPK cascade proteins including ERK 1/2 and p38 MAPK (Schonwasser *et al.* 1998). p38 MAPK plays a major role in the LPS-activated BV2 microglia while ERK 1/2 plays a major role in the IFN-γ activated BV2 microglia (Kim *et al.* 2004; Park *et al.* 2005). Based on these results, we can speculate that aripiprazole may inhibit IFN-γ-induced microglial activation through the suppression of IFN-γ-induced elevation of $[Ca^{2+}]_i$ in microglia. The effect of aripiprazole on Ca^{2+} regulation shown in the present study is interesting because Ca^{2+} signaling dysfunction is proposed for the central unifying molecular pathology in schizophrenia (Lidow 2003). However, aripiprazole may modulate the expression of other factors that act upstream of calcium to dampen IFN-γ- induced signaling.

Labuzek *et al.* reported that chlorpromazine and loxapine, antipsychotics with D_2 receptor antagonism, had inhibitory effect, while, quinpirole, D_2 receptor full agonist, had little effect on the inflammatory cytokine release from LPS-activated rat primary microglia. They therefore suggested that microglia might not have functional dopaminergic receptors (Labuzek *et al.* 2005). However, Faber *et al.* provided the first evidence for the existence of functional dopaminergic receptors on rat primary microglia. In their study, quinpirole inhibited the release of NO from LPS-activated microglia (Farber *et al.* 2005). Hou *et al.* reported that even antipsychotics, all of which have D2 antagonism, had different effects on LPS-induced mouse N9 microglial activation. In their study, not either haloperidol or clozapine, but only olanzapine had an inhibitory effect on LPS-induced microglial activation. We recently reported that not haloperidol but several atypical antipsychotics, all of which have D2 antagonism, demonstrated a significantly inhibitory effect on IFN-γ–induced 6-3 microglial activation (Kato *et al.* 2007; Bian *et al.* 2008). In the present study, RT-PCR revealed the

existence of dopamine D_2 receptors while not quinpirole but aripiprazole demonstrated an inhibitory effect on NO release from IFN-γ- or LPS- activated 6-3 microglia. These results seem to suggest that the dopamine D_2 receptors may not be involved in IFN-γ- or LPS- induced microglial activation. Aripiprazole has recently been reported to exert D_2-receptor-mediated MAPK phosphorylation in transfected CHO cells (Bruins Slot *et al.* 2006; Urban *et al.* 2007). Therefore, the expression of the protein levels of dopamine D_2 receptors as well as the functions of these receptors should be investigated to confirm the above speculations. Aripiprazole is also known to be both $5HT_{1A}$ agonist and $5HT_{2A}$ antagonist (Burris *et al.* 2002). Serotoninergic receptors might, therefore, be involved in the inhibitory effect of aripiprazole on IFN-γ-induced microglial activation. Microglia is known to express many kinds of neurotransmitter receptors including glutamatergic, GABAergic, purinergic, dopaminergic, cholinergic, adrenergic, and cannabinoid receptors (Pocock and Kettenmann 2007). However, to the best of our knowledge regarding serotonin receptors, there have been no reports regarding the expression of $5HT_{1A}$ or $5HT_{2A}$ receptors in the microglia, only one report for the existence of $5\text{-}HT_7$ in human microglial cells (Mahe *et al.* 2005). Atypical antipsychotics can have a positive effect on cell growth and survival through unique signaling pathways (Lu and Dwyer 2005). Therefore, the pharmacological basis for their effects does not appear to be directly related to only the dopaminergic and serotoninergic receptors.

Lipopolysaccharide is usually used as an activator of the microglia. LPS is a major constituent of the cell wall in gram negative bacteria and it is thus suitable to provide especially bacterial inflammatory reactions. However, there has been little evidence so far regarding the relationship between schizophrenia and bacterial infections. On the other hand, there have been some reports that suggested the relationship between schizophrenia and IFN-γ, a major immuno-activator in the CNS. IFN-γ is released by infiltrating T cells as well as from activated microglia in the CNS (Kawanokuchi *et al.* 2006). The most important immunological studies in schizophrenia have shown a shift from Th1-like cellular to Th2-like humoral immune reactivity and these studies have suggested a blunted IFN-γ signal in schizophrenia (Schwarz *et al.* 2001a,b). However, Rothermundt *et al.* have argued that the reduced IFN-γ production *in vitro* may reflect an increased production *in vivo*, as observed in several autoimmune disorders (Rothermundt *et al.* 2001). Furthermore, the serum levels of IL-2 and IFN-γ, and the production of these cytokines from peripheral blood mononuclear cells stimulated by phytohemagglutinin has been reported to be significantly higher in patients with schizophrenia than in controls (Cazzullo *et al.* 2001, 2002). We thus used IFN-γ as wells as LPS as an activator of microglia. Takeuchi *et al.* recently demonstrated that IFN-γ induced microglial-activation-induced cell death for the chronic treatment (Takeuchi *et al.* 2006). However, under the present experimental conditions, IFN-γ treatment did not have any effect on the cell viability of microglia.

The typical dose range of aripiprazole is 10–30 mg/day and the typical serum concentration or plasma range of aripiprazole is 0–1000 ng/mL (Alexopoulos *et al.* 2004; Chew *et al.* 2006). Antipsychotics are known to accumulate in brain tissue to levels that are 25–30 fold higher than serum levels (Baumann *et al.* 2004). Therefore, in spite of no evidence that the effect of a drug in cell culture could be compared to the effect of the same drug at a brain tissue level even in the same range of concentration, the concentrations of aripiprazole used in the present study might thus not be substantially different from the brain tissue levels for aripiprazole.

A recent post-mortem brain study has indicated a close relationship between schizophrenia and neurogenesis (Reif *et al.* 2006). Clozapine, olanzapine and risperidone have been reported to stimulate neurogenesis *in vivo* (Wakade *et al.* 2002; Halim *et al.* 2004; Wang *et al.* 2004). However, the direct effect of antipsychotics on the neurosphere have recently been reported to be limited (Councill *et al.* 2006). Inflammatory cytokines and NO have reported to have an inhibitory effect on neurogenesis (Monje *et al.* 2003; Cardenas *et al.* 2005; Iosif *et al.* 2006; Kaneko *et al.* 2006). Aripiprazole may thus indirectly stimulate neurogenesis through the inhibition of the microglia-derived release of inflammatory cytokines and NO.

Structural imaging studies, as well as gene expression studies and evidence for the dysfunction of myelin and oligodendrocyte, have suggested the presence of abnormalities of white matter in schizophrenia (Hakak *et al.* 2001; Davis *et al.* 2003; Uranova *et al.* 2004; Schlosser *et al.* 2007). Microglial activation in the CNS has been implicated in the pathogenesis of white matter disorders. Activated microglia has reported to induce cytotoxicity of oligodendrocytes via the release of NO, peroxynitrite and inflammatory cytokines such as TNF-α (Merrill *et al.* 1993; Buntinx *et al.* 2004; Li *et al.* 2005). Therefore, the present results suggest that aripiprazole may ameliorate white matter disorders via inhibiting microglial activation in the brain of patients with schizophrenia.

The present study demonstrated that not only atypical antipsychotics which have dopamine D_2 receptor antagonism but also aripiprazole have significantly anti-inflammatory effects via the inhibition of microglial activation. Our results might therefore shed some new light on the understanding of the pathophysiology of schizophrenia and the therapeutic strategies for the treatment of schizophrenia with anti-inflammatory/immunosuppressive agents. For further studies, the more detailed molecular mechanism of the inhibitory effect of aripiprazole on microglial activation should be clarified while *in vivo* studies to confirm the present results should also be performed.

Acknowledgements

The present study was supported partly by a grant-in-aid from the Japan Society for the Promotion of Science. The authors thank Prof. Makoto Sawada of Nagoya University for providing us with the microglial cell line, 6-3. The authors also thank Dr. Makiko Kido, Shuji Fukagawa and Leo Gotoh of Kyushu University for valuable technical advices.

Contributors

All authors contributed substantially to the scientific process leading up to the writing of the present paper. AM, the principal investigator of the present research, and TK made the conception and design of the project and wrote the protocol. The performance of experiments and the analysis and interpretation of data were done by TK, YM, HH, SS, YS and SH. TK wrote the first draft of the manuscript. The critical revision of the manuscript was made by IT and SK. All authors contributed to and have approved the final manuscript.

References

Akhondzadeh S., Tabatabaee M., Amini H., Ahmadi Abhari S. A., Abbasi S. H. and Behnam B. (2007) Celecoxib as adjunctive therapy in schizophrenia: a double-blind, randomized and placebo-controlled trial. *Schizophr. Res.* **90**, 179–185.

Alexopoulos G. S., Streim J., Carpenter D. and Docherty J. P. (2004) Using antipsychotic agents in older patients. *J. Clin. Psychiatry* **65**(Suppl 2), 5–104.

Baumann P., Hiemke C., Ulrich S. *et al.* and Arbeitsge-meinschaft fur neuropsychopharmakologie und p. (2004) The AGNP-TDM expert group consensus guidelines: therapeutic drug monitoring in psychiatry. *Pharmacopsychiatry* **37**, 243–265.

Bayer T. A., Buslei R., Havas L. and Falkai P. (1999) Evidence for activation of microglia in patients with psychiatric illnesses. *Neurosci. Lett.* **271**, 126–128.

Bernstein H. G., Bogerts B. and Keilhoff G. (2005) The many faces of nitric oxide in schizophrenia. A review. *Schizophr. Res.* **78**, 69–86.

Bian Q., Kato T., Monji A., Hashioka S., Mizoguchi Y., Horikawa H. and Kanba S. (2008) The effect of atypical antipsychotics, perospirone, ziprasidone and quetiapine on microglial activation induced by interferon-gamma. *Prog. Neuropsychopharmacol. Biol. Psychiatry* **32**, 42–48.

Bruins Slot L. A., De Vries L., Newman-Tancredi A. and Cussac D. (2006) Differential profile of antipsychotics at serotonin 5-HT1A and dopamine D2S receptors coupled to extracellular signal-regulated kinase. *Eur. J. Pharmacol.* **534**, 63–70.

Buntinx M., Moreels M., Vandenabeele F., Lambrichts I., Raus J., Steels P., Stinissen P. and Ameloot M. (2004) Cytokine-induced cell death in human oligodendroglial cell lines: I. Synergistic effects of IFN-gamma and TNF-alpha on apoptosis. *J. Neurosci. Res.* **76**, 834–845.

Burris K. D., Molski T. F., Xu C., Ryan E., Tottori K., Kikuchi T., Yocca F. D. and Molinoff P. B. (2002) Aripiprazole, a novel antipsychotic, is a high-affinity partial agonist at human dopamine D2 receptors. *J. Pharmacol. Exp. Ther.* **302**, 381–389.

Cardenas A., Moro M. A., Hurtado O., Leza J. C. and Lizasoain I. (2005) Dual role of nitric oxide in adult neurogenesis. *Brain Res. Brain Res. Rev.* **50**, 1–6.

Cazzullo C. L., Sacchetti E., Galluzzo A., Panariello A., Colombo F., Zagliani A. and Clerici M. (2001) Cytokine profiles in drug-naive schizophrenic patients. *Schizophr. Res.* **47**, 293–298.

Cazzullo C. L., Sacchetti E., Galluzzo A. *et al.* (2002) Cytokine profiles in schizophrenic patients treated with risperidone: a 3-month follow-up study. *Prog. Neuropsychopharmacol. Biol. Psychiatry* **26**, 33–39.

Chew M. L., Mulsant B. H., Pollock B. G., Lehman M. E., Greenspan A., Kirshner M. A., Bies R. R., Kapur S. and Gharabawi G. (2006) A model of anticholinergic activity of atypical antipsychotic medications. *Schizophr. Res.* **88**, 63–72.

Councill J. H., Tucker E. S., Haskell G. T., Maynard T. M., Meechan D. W., Hamer R. M., Lieberman J. A. and LaMantia A. S. (2006) Limited influence of olanzapine on adult forebrain neural precursors in vitro. *Neuroscience* **140**, 111–122.

Davis K. L., Stewart D. G., Friedman J. I., Buchsbaum M., Harvey P. D., Hof P. R., Buxbaum J. and Haroutunian V. (2003) White matter changes in schizophrenia: evidence for myelin-related dysfunction. *Arch. Gen. Psychiatry* **60**, 443–456.

Drzyzga L., Obuchowicz E., Marcinowska A. and Herman Z. S. (2006) Cytokines in schizophrenia and the effects of antipsychotic drugs. *Brain Behav. Immun.* **20**, 532–545.

Farber K., Pannasch U. and Kettenmann H. (2005) Dopamine and noradrenaline control distinct functions in rodent microglial cells. *Mol. Cell. Neurosci.* **29**, 128–138.

Franciosi S., Choi H. B., Kim S. U. and McLarnon J. G. (2002) Interferon-gamma acutely induces calcium influx in human microglia. *J. Neurosci. Res.* **69**, 607–613.

Grynkiewicz G., Poenie M. and Tsien R. Y. (1985) A new generation of Ca2+ indicators with greatly improved fluorescence properties. *J. Biol. Chem.* **260**, 3440–3450.

Hakak Y., Walker J. R., Li C., Wong W. H., Davis K. L., Buxbaum J. D., Haroutunian V. and Fienberg A. A. (2001) Genome-wide expression analysis reveals dysregulation of myelination-related genes in chronic schizophrenia. *Proc. Natl Acad. Sci. USA* **98**, 4746–4751.

Halim N. D., Weickert C. S., McClintock B. W., Weinberger D. R. and Lipska B. K. (2004) Effects of chronic haloperidol and clozapine treatment on neurogenesis in the adult rat hippocampus. *Neuropsychopharmacology* **29**, 1063–1069.

Hoffmann A., Kann O., Ohlemeyer C., Hanisch U. K. and Kettenmann H. (2003) Elevation of basal intracellular calcium as a central element in the activation of brain macrophages (microglia): suppression of receptor-evoked calcium signaling and control of release function. *J. Neurosci.* **23**, 4410–4419.

Iosif R. E., Ekdahl C. T., Ahlenius H., Pronk C. J., Bonde S., Kokaia Z., Jacobsen S. E. and Lindvall O. (2006) Tumor necrosis factor receptor 1 is a negative regulator of progenitor proliferation in adult hippocampal neurogenesis. *J. Neurosci.* **26**, 9703–9712.

Kane J. M., Crandall D. T., Marcus R. N., Eudicone J., Pikalov C. and Wh S. (2007) Symptomatic remission in schizophrenia patients treated with aripiprazole or haloperidol for up to 52 weeks. *Schizophr. Res.* **95**, 143–150.

Kaneko N., Kudo K., Mabuchi T., Takemoto K., Fujimaki K., Wati H., Iguchi H., Tezuka H. and Kanba S. (2006) Suppression of cell proliferation by interferon-alpha through interleukin-1 production in adult rat dentate gyrus. *Neuropsychopharmacology* **31**, 2619–2626.

Kanzawa T., Sawada M., Kato K., Yamamoto K., Mori H. and Tanaka R. (2000) Differentiated regulation of allo-antigen presentation by different types of murine microglial cell lines. *J. Neurosci. Res.* **62**, 383–388.

Kapur S. and Mamo D. (2003) Half a century of antipsychotics and still a central role for dopamine D2 receptors. *Prog. Neuropsychopharmacol. Biol. Psychiatry* **27**, 1081–1090.

Kato T., Monji A., Hashioka S. and Kanba S. (2007) Risperidone significantly inhibits interferon-gamma-induced microglial activation in vitro. *Schizophr. Res.* **92**, 108–115.

Kawanokuchi J., Mizuno T., Takeuchi H., Kato H., Wang J., Mitsuma N. and Suzumura A. (2006) Production of interferon-gamma by microglia. *Mult. Scler.* **12**, 558–564.

Kim H. S., Whang S. Y., Woo M. S., Park J. S., Kim W. K. and Han I. O. (2004) Sodium butyrate suppresses interferon-gamma-, but not lipopolysaccharide-mediated induction of nitric oxide and tumor necrosis factor-alpha in microglia. *J. Neuroimmunol.* **151**, 85–93.

Labuzek K., Kowalski J., Gabryel B. and Herman Z. S. (2005) Chlorpromazine and loxapine reduce interleukin-1beta and interleukin-2 release by rat mixed glial and microglial cell cultures. *Eur. Neuropsychopharmacol.* **15**, 23–30.

Lemmer K., Ahnert-Hilger G., Hopfner M., Hoegerle S., Faiss S., Grabowski P., Jockers-Scherubl M., Riecken E. O., Zeitz M. and Scherubl H. (2002) Expression of dopamine receptors and transporter in neuroendocrine gastrointestinal tumor cells. *Life Sci.* **71**, 667–678.

Li J., Baud O., Vartanian T., Volpe J. J. and Rosenberg P. A. (2005) Peroxynitrite generated by inducible nitric oxide synthase and NADPH oxidase mediates microglial toxicity to oligodendrocytes. *Proc. Natl Acad. Sci. USA* **102**, 9936–9941.

Lidow M. S. (2003) Calcium signaling dysfunction in schizophrenia: a unifying approach. *Brain Res. Brain Res. Rev.* **43**, 70–84.

Lieberman J. A. (1999) Is schizophrenia a neurodegenerative disorder? A clinical and neurobiological perspective *Biol. Psychiatry* **46**, 729–739.

Lieberman J. A., Tollefson G. D., Charles C. *et al.* (2005) Antipsychotic drug effects on brain morphology in first-episode psychosis. *Arch. Gen. Psychiatry* **62**, 361–370.

Lin A., Kenis G., Bignotti S., Tura G. J., De Jong R., Bosmans E., Pioli R., Altamura C., Scharpe S. and Maes M. (1998) The inflammatory response system in treatment-resistant schizophrenia: increased serum interleukin-6. *Schizophr. Res.* **32**, 9–15.

Lu X. H. and Dwyer D. S. (2005) Second-generation antipsychotic drugs, olanzapine, quetiapine, and clozapine enhance neurite outgrowth in PC12 cells via PI3K/AKT, ERK, and pertussis toxin-sensitive pathways. *J. Mol. Neurosci.* **27**, 43–64.

Lu L. X., Guo S. Q., Chen W., Li Q., Cheng J. and Guo J. H. (2004) Effect of clozapine and risperidone on serum cytokine levels in patients with first-episode paranoid schizophrenia. *Di Yi Jun Yi Da Xue Xue Bao* **24**, 1251–1254.

Mahe C., Loetscher E., Dev K. K., Bobirnac I., Otten U. and Schoeffter P. (2005) Serotonin 5-HT7 receptors coupled to induction of interleukin-6 in human microglial MC-3 cells. *Neuropharmacology* **49**, 40–47.

McGeer P. L., Kawamata T., Walker D. G., Akiyama H., Tooyama I. and McGeer E. G. (1993) Microglia in degenerative neurological disease. *Glia* **7**, 84–92.

Merrill J. E., Ignarro L. J., Sherman M. P., Melinek J. and Lane T. E. (1993) Microglial cell cytotoxicity of oligodendrocytes is mediated through nitric oxide. *J. Immunol.* **151**, 2132–2141.

Miyamoto S., Duncan G. E., Marx C. E. and Lieberman J. A. (2005) Treatments for schizophrenia: a critical review of pharmacology and mechanisms of action of antipsychotic drugs. *Mol. Psychiatry* **10**, 79–104.

Miyaoka T., Yasukawa R., Yasuda H., Hayashida M., Inagaki T. and Horiguchi J. (2007) Possible antipsychotic effects of minocycline in patients with schizophrenia. *Prog. Neuropsychopharmacol. Biol. Psychiatry* **31**, 304–307.

Mizoguchi Y., Monji A. and Nabekura J. (2002) Brain-derived neurotrophic factor induces long-lasting Ca2+-activated K+ currents in rat visual cortex neurons. *Eur. J. Neurosci.* **16**, 1417–1424.

Monje M. L., Toda H. and Palmer T. D. (2003) Inflammatory blockade restores adult hippocampal neurogenesis. *Science* **302**, 1760–1765.

Nikodemova M., Duncan I. D. and Watters J. J. (2006) Minocycline exerts inhibitory effects on multiple mitogen-activated protein kinases and IkappaBalpha degradation in a stimulus-specific manner in microglia. *J. Neurochem.* **96**, 314–323.

Park J. S., Woo M. S., Kim S. Y., Kim W. K. and Kim H. S. (2005) Repression of interferon-gamma-induced inducible nitric oxide synthase (iNOS) gene expression in microglia by sodium butyrate is mediated through specific inhibition of ERK signaling pathways. *J. Neuroimmunol.* **168**, 56–64.

Pocock J. M. and Kettenmann H. (2007) Neurotransmitter receptors on microglia. *Trends Neurosci.* **30**, 527–535.

Potkin S. G., Saha A. R., Kujawa M. J., Carson W. H., Ali M., Stock E., Stringfellow J., Ingenito G. and Marder S. R. (2003) Aripiprazole, an antipsychotic with a novel mechanism of action, and risperidone vs placebo in patients with schizophrenia and schizoaffective disorder. *Arch. Gen. Psychiatry* **60**, 681–690.

Radewicz K., Garey L. J., Gentleman S. M. and Reynolds R. (2000) Increase in HLA-DR immunoreactive microglia in frontal and temporal cortex of chronic schizophrenics. *J. Neuropathol. Exp. Neurol.* **59**, 137–150.

Reif A., Fritzen S., Finger M., Strobel A., Lauer M., Schmitt A. and Lesch K. P. (2006) Neural stem cell proliferation is decreased in schizophrenia, but not in depression. *Mol. Psychiatry* **11**, 514–522.

Rothermundt M., Arolt V. and Bayer T. A. (2001) Review of immunological and immunopathological findings in schizophrenia. *Brain Behav. Immun.* **15**, 319–339.

Salisbury D. F., Kuroki N., Kasai K., Shenton M. E. and McCarley R. W. (2007) Progressive and interrelated functional and structural evidence of post-onset brain reduction in schizophrenia. *Arch. Gen. Psychiatry* **64**, 521–529.

Sawada M., Imai F., Suzuki H., Hayakawa M., Kanno T. and Nagatsu T. (1998) Brain-specific gene expression by immortalized microglial cell-mediated gene transfer in the mammalian brain. *FEBS Lett.* **433**, 37–40.

Schlosser R. G., Nenadic I., Wagner G. *et al.* (2007) White matter abnormalities and brain activation in schizophrenia: a combined DTI and fMRI study. *Schizophr. Res.* **89**, 1–11.

Schonwasser D. C., Marais R. M., Marshall C. J. and Parker P. J. (1998) Activation of the mitogen-activated protein kinase/extracellular signal-regulated kinase pathway by conventional, novel, and atypical protein kinase C isotypes. *Mol. Cell. Biol.* **18**, 790–798.

Schwarz M. J., Muller N., Riedel M. and Ackenheil M. (2001a) The Th2-hypothesis of schizophrenia: a strategy to identify a subgroup of schizophrenia caused by immune mechanisms. *Med. Hypotheses* **56**, 483–486.

Schwarz M. J., Chiang S., Muller N. and Ackenheil M. (2001b) T-helper-1 and T-helper-2 responses in psychiatric disorders. *Brain Behav. Immun.* **15**, 340–370.

Shapiro D. A., Renock S., Arrington E., Chiodo L. A., Liu L. X., Sibley D. R., Roth B. L. and Mailman R. (2003) Aripiprazole, a novel atypical antipsychotic drug with a unique and robust pharmacology. *Neuropsychopharmacology* **28**, 1400–1411.

Steiner J., Mawrin C., Ziegeler A., Bielau H., Ullrich O., Bernstein H. G. and Bogerts B. (2006) Distribution of HLA-DR-positive microglia in schizophrenia reflects impaired cerebral lateralization. *Acta Neuropathol.* **112**, 305–316.

Steiner J., Bielau H., Brisch R., Danos P., Ullrich O., Mawrin C., Bernstein H. G. and Bogerts B. (2008) Immunological aspects in the neurobiology of suicide: elevated microglial density in schizophrenia and depression is associated with suicide. *J. Psychiatr. Res.* **42**, 151–157.

Stoll G. and Jander S. (1999) The role of microglia and macrophages in the pathophysiology of the CNS. *Prog. Neurobiol.* **58**, 233–247.

Takeuchi H., Wang J., Kawanokuchi J., Mitsuma N., Mizuno T. and Suzumura A. (2006) Interferon-gamma induces microglial-activation-induced cell death: a hypothetical mechanism of relapse and remission in multiple sclerosis. *Neurobiol. Dis.* **22**, 33–39.

Tandon R., Marcus R. N., Stock E. G., Riera L. C., Kostic D., Pans M., McQuade R. D., Nyilas M., Iwamoto T. and Crandall D. T. (2006) A prospective, multicenter, randomized, parallel-group, open-label study of aripiprazole in the management of patients with schizophrenia or schizoaffective disorder in general psychiatric practice: Broad Effectiveness Trial With Aripiprazole (BETA). *Schizophr. Res.* **84**, 77–89.

Taylor D., Atkinson J., Fischetti C., Sparshatt A. and Jones S. (2007) A prospective 6-month analysis of the naturalistic use of aripiprazole - factors predicting favourable outcome. *Acta Psychiatr. Scand.* **116**, 461–466.

Uranova N. A., Vostrikov V. M., Orlovskaya D. D. and Rachmanova V. I. (2004) Oligodendroglial density in the prefrontal cortex in schizophrenia and mood disorders: a study from the Stanley Neuropathology Consortium. *Schizophr. Res.* **67**, 269–275.

Urban J. D., Vargas G. A., von Zastrow M. and Mailman R. B. (2007) Aripiprazole has functionally selective actions at dopamine D2 receptor-mediated signaling pathways. *Neuropsychopharmacology* **32**, 67–77.

Wakade C. G., Mahadik S. P., Waller J. L. and Chiu F. C. (2002) Atypical neuroleptics stimulate neurogenesis in adult rat brain. *J. Neurosci. Res.* **69**, 72–79.

Wang H. D., Dunnavant F. D., Jarman T. and Deutch A. Y. (2004) Effects of antipsychotic drugs on neurogenesis in the forebrain of the adult rat. *Neuropsychopharmacology* **29**, 1230–1238.

Zhang X. Y., Zhou D. F., Cao L. Y., Zhang P. Y., Wu G. Y. and Shen Y. C. (2004) Changes in serum interleukin-2, -6, and -8 levels before and during treatment with risperidone and haloperidol: relationship to outcome in schizophrenia. *J. Clin. Psychiatry* **65**, 940–947.

Cell Death and Differentiation (2008), 1–11

www.nature.com/cdd

Galectin-1 promotes basal and kainate-induced proliferation of neural progenitors in the dentate gyrus of adult mouse hippocampus

K Kajitani[1,2], H Nomaru[1], M Ifuku[3], N Yutsudo[1], Y Dan[1], T Miura[1,2], D Tsuchimoto[1], K Sakumi[1], T Kadoya[4], H Horie[5], F Poirier[6], M Noda[3] and Y Nakabeppu*[,1]

We examined the expression of galectin-1, an endogenous lectin with one carbohydrate-binding domain, in the adult mouse hippocampus after systemic kainate administration. We found that the expression of galectin-1 was remarkably increased in activated astrocytes of the CA3 subregion and dentate gyrus of the hippocampus, and in nestin-positive neural progenitors in the dentate gyrus. Quantitative reverse transcription PCR (RT-PCR) analysis revealed that the galectin-1 mRNA level in hippocampus began to increase 1 day after kainate administration and that a 13-fold increase was attained within 3 days. Western blotting analysis confirmed that the level of galectin-1 protein increased to more than three-fold a week after the exposure. We showed that isolated astrocytes express and secrete galectin-1. To clarify the significance of the increased expression of galectin-1 in hippocampus, we compared the levels of hippocampal cell proliferation in galectin-1 knockout and wild-type mice after saline or kainate administration. The number of 5-bromo-2′-deoxyuridine (BrdU)-positive cells detected in the subgranular zone (SGZ) of galectin-1 knockout mice decreased to 62% with saline, and to 52% with kainate, as compared with the number seen in the wild-type mice. Most of the BrdU-positive cells in SGZ expressed doublecortin and neuron-specific nuclear protein, indicating that they are immature neurons. We therefore concluded that galectin-1 promotes basal and kainate-induced proliferation of neural progenitors in the hippocampus.
Cell Death and Differentiation advance online publication, 14 November 2008; doi:10.1038/cdd.2008.162

Neurons are expected to survive and function throughout the lifespan of an individual; however, they are postmitotic and no longer proliferative, and are inevitably eliminated as a consequence of damage accumulated during aging.[1] It is considered that there must be multiple mechanisms for maintaining neural networks in adult brains, including neurogenesis by which new neurons are supplied in restricted areas.[2,3]

It has been established that adult neurogenesis in rodents is enhanced after brain insults caused by ischemia[4] and epileptic seizure.[5] Insult to the brain likely triggers signals that activate expression of a set of genes, known as immediate early genes, in the hippocampus and cerebral cortex.[6] Among many immediate early gene products, Jun and Fos family proteins function as components of transcription factor activator protein-1 complexes,[7,8] and thus regulate transcription of various genes involved in cell proliferation, differentiation, and programmed cell death.[6] We reported earlier that ΔFosB, an activator protein-1 subunit encoded by an alternatively spliced form of *fosB* transcript, triggers quiescent cells to transit G1, initiate DNA replication, and ultimately undergo cell division, followed by such fates as proliferation, differentiation, and programmed cell death.[9–12] ΔFosB is known to be chronically expressed in the dentate gyrus of hippocampus after ischemia, which is where and when neurogenesis takes place.[13] We identified earlier a downstream target upregulated by ΔFosB, termed galectin-1, one of the major β-galactoside sugar-binding lectins in mammals.[11] We further showed that this lectin regulates such cell fates as cell proliferation, differentiation, and death, as does ΔFosB.[12–14] We thus consider that galectin-1 may also be involved in the regulation of neural cell fate.[15]

Galectin-1 is a ubiquitously expressed 14.5-kDa protein with a single carbohydrate-binding domain, and is a multifunctional

[1]Division of Neurofunctional Genomics, Department of Immunobiology and Neuroscience, Medical Institute of Bioregulation, Kyushu University, Fukuoka, Japan; [2]Department of Neuropsychiatry, Graduate School of Medical Sciences, Kyushu University, Fukuoka, Japan; [3]Laboratory of Pathophysiology, Graduate School of Pharmaceutical Sciences, Kyushu University, Fukuoka, Japan; [4]CMC R&D Laboratories, Kirin Pharma Co., Ltd., Takasaki, Japan; [5]Research Center of Brain and Oral Science, Kanagawa Dental College, Yokosuka, Japan and [6]The Department of Developmental Biology, Institute Jacques Monod, Universities Paris 6 and Paris 7, Paris, France

*Corresponding author: Y Nakabeppu, Division of Neurofunctional Genomics, Department of Immunobiology and Neuroscience, Medical Institute of Bioregulation, Kyushu University, 3-1-1 Maidashi, Higashi-Ku, Fukuoka 812-8582, Japan.
Tel: +81 92 642 6800; Fax: +81 92 642 6791; E-mail: yusaku@bioreg.kyushu-u.ac.jp
Keywords: galectin-1; adult neurogenesis; kainate; hippocampus; knockout mice; astrocyte
Abbreviations: BrdU, 5-bromo-2′-deoxyuridine; DCX, doublecortin; GCL, granule cell layer; GFAP, glial fibrillary acidic protein; IHC, immunohistochemistry; NeuN, neuron-specific nuclear protein; PSA-NCAM, polysialylated neural cell adhesion molecule; SGZ, subgranular zone; SVZ, subventricular zone
Received 17.9.08; revised 06.10.08; accepted 12.10.08; Edited by P Vandenabeele

molecule involved in the regulation of cell adhesion, cell proliferation, and programmed cell death.[16–18] Galectin-1 is known to be involved in the growth and/or guidance of primary sensory olfactory axons, indicating that it plays a role in neural pathfinding in the mammalian nervous system.[19] Furthermore, galectin-1 promotes axonal regeneration after axotomy in peripheral nerves of rat,[20] suggesting that this lectin may participate in response to brain insult.

In this study, we examined the expression level of galectin-1 in the adult mouse hippocampus after systemic administration of kainate, an agent that produces epileptic seizures and enhances neurogenesis, in order to examine the role of galectin-1 in response to brain insult. Furthermore, we compared the extent of proliferation of neural progenitors in galectin-1 knockout and wild-type mice after kainate exposure.

Results

Systemic administration of kainate induces the expression of galectin-1 in the adult mouse hippocampus. To evaluate the expression of galectin-1 after brain insult, 10-week-old C57BL/6J mice were injected intraperitoneally with kainate (30 mg/kg) and were killed 1 week after injection. The brain sections were then prepared and subjected to immunohistochemistry (IHC). In the untreated mice, the expression of galectin-1 was detected in soma and, to a lesser extent, in neurites of large round neurons scattered in the hippocampus (Figure 1a–c). After 1 week of kainate administration, the population of galectin-1-positive cells was significantly increased in the hippocampus, especially in the CA3 subregion and, to a lesser extent, in the dentate gyrus (Figure 1d–f). The immunoreactive signals were not observed in galectin-1 knockout mice with or without kainate administration (Supplementary Figure S1). We thus concluded that the expression of galectin-1 is inducible in the brain after kainate administration. In the CA3 subregion of the mouse hippocampus, the predominant expression of galectin-1 was observed in cells with multiple

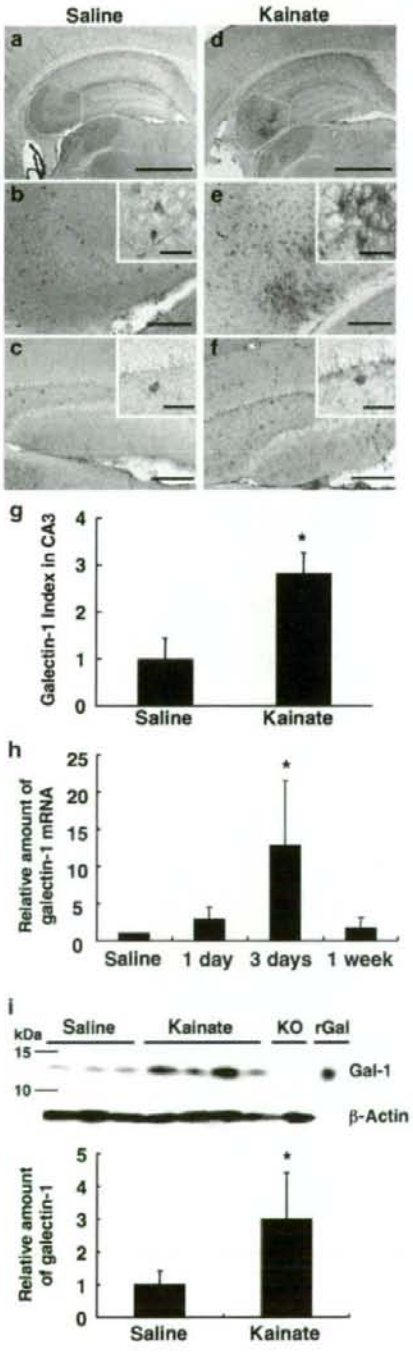

Figure 1 Kainate-induced expression of galectin-1. (**a–f**) Immunohistochemical detection of galectin-1. Mouse brain sections were prepared 1 week after kainate administration (kainate), and were subjected to IHC to detect galectin-1. Untreated mice (saline) were injected with saline instead of kainate. Scale bars: **a** and **d**, 1 mm; **b**, **c**, **e** and **f**, 200 μm; inset, 50 μm. (**g**) Quantitative analysis of galectin-1 expression induced after the exposure to kainate. Galectin-1 immunoreactivity in the CA3 subregion as shown in the dotted area in panels a and d relative to the value of the untreated group (saline) is shown as a bar graph with the mean ± SD (saline-injected mice, $N=4$; kainate-injected mice, $N=5$). Unpaired *t*-test, $^*P<0.01$. (**h**) Real-time RT-PCR analysis of galectin-1 mRNA. RNA was isolated from the dissected hippocampus at the indicated times after the injection of mice with kainate or 1 week after saline injection (saline), and was then subjected to real-time RT-PCR for galectin-1 (Gal-1) and GAPDH mRNA. The amount of galectin-1 mRNA determined by RT-PCR was normalized with that of GAPDH mRNA at each time point and the amount of the mRNA relative to that of the untreated group is shown in the bar graph as a mean ± SD. Unpaired *t*-test, $^*P<0.05$. ($N=3$ mice per group). (**i**) Western blotting analysis of galectin-1 protein. Whole cell extracts of the mouse hippocampus obtained 1 week after kainate administration were subjected to western blotting analysis for galectin-1 (Gal-1) and β-actin. KO, an extract from a galectin-1 knockout mouse; rGal, recombinant mouse galectin-1.[14] The amount of galectin-1 protein determined by western blotting was normalized with that of β-actin, and the mean value of the amount of galectin-1 relative to that of the untreated group (saline) is shown in the bar graph with the mean ± SD. The control mice injected with saline ($N=3$) and kainate-injected mice ($N=4$ mice). Unpaired *t*-test, $^*P<0.01$

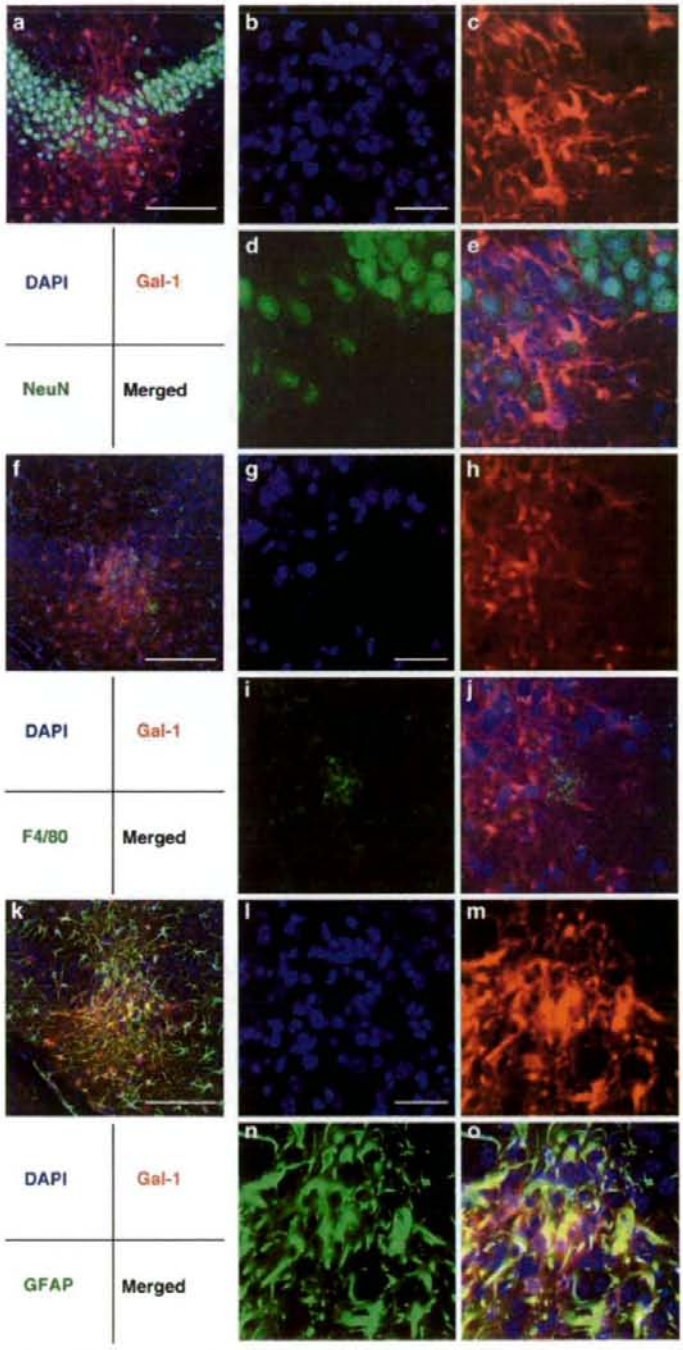

Figure 2 Kainate administration induces the expression of galectin-1 in activated astrocytes in the CA3 subregion of mouse hippocampus. Mouse brain sections were prepared a week after kainate administration, and were subjected to multi-immunofluorescence microscopy with a laser scanning confocal microscope. (**a**–**e**) Expression of galectin-1 in neurons. Blue, DAPI; red, galectin-1 (Gal-1); and green, NeuN. (**f**–**j**) Expression of galectin-1 in microglias. Blue, DAPI; red, galectin-1 (Gal-1); green, F4/80. (**k**–**o**) Expression of galectin-1 in astrocytes. Blue, DAPI; red, galectin-1 (Gal-1); and green, GFAP. Scale bars: **a**, **f** and **k**, 200 μm; **b**–**l**, **g**–**j** and **l**–**o**, 50 μm

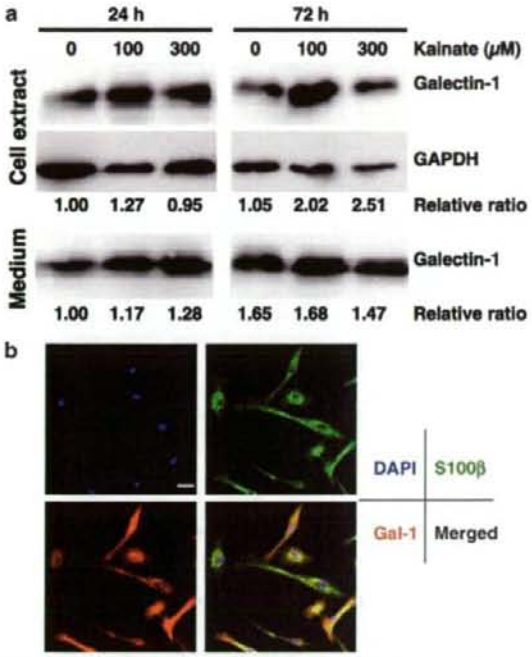

Figure 3 Isolated primary astrocytes express and secrete galectin-1 *in vitro*. (**a**) Astrocytes isolated from the cerebral cortex obtained from neonatal C57BL/6J mice were kept in a serum-free medium containing 0, 100, and 300 μM kainate for 24 or 72 h. After exposure to kainate, cell extracts from cultured astrocytes and conditioned media were collected and were subjected to western blotting using anti-rhGal-1. Upper panel: galectin-1 from cell extracts, middle panel: GAPDH from cell extracts, lower panel: galectin-1 in conditioned media. The amount of galectin-1 protein determined by western blotting was normalized with that of GAPDH. ($N = 3$ per group). The amount of galectin-1 in conditioned media is indicated relative to that of the sample without kainate exposure at 24 h ($N = 3$ per group). (**b**) Galectin-1 expression in cultured astrocytes. Cultured astrocytes were subjected to immunofluorescence confocal microscopy with anti-rhGal-1 and anti-S100β. Blue, DAPI; red, galectin-1 (Gal-1); and green, S100β. Scale bar = 40 μm

stellate processes, especially in their soma and processes (Figure 1e, inset). Intensities of galectin-1 immunoreactivity in the CA3 subregion were increased about three-fold 1 week after kainate administration (Figure 1g).

To evaluate the level of galectin-1 mRNA in the hippocampus, we performed quantitative real-time reverse transcription PCR (RT-PCR). The relative expression level of galectin-1 mRNA began to increase 1 day after kainate administration, and peaked at a level that was 13-fold higher than that of the untreated group 3 days after the exposure (Figure 1h). A 14.5-kDa galectin-1 protein, which exhibited the same mobility as the recombinant mouse galectin-1 protein, was detected in wild-type but not in galectin-1 knockout mice samples, and the level of galectin-1 protein reached a three-fold higher level 1 week after the exposure, as compared with the level seen in the untreated group (Figure 1i). We thus concluded that the systemic administration of kainate resulted in an increase in galectin-1 gene expression and the accumulation of galectin-1 protein in the adult mouse hippocampus.

Systemic administration of kainate induces the expression of galectin-1 in activated astrocytes in the CA3 subregion of mouse hippocampus. After kainate administration, galectin-1 immunoreactivity in the CA3 subregion was not detected in either neuron-specific nuclear protein (NeuN)-positive pyramidal neurons (Figure 2a–e) or microglia with F4/80 immunoreactivity, whose level reached a maximum at 12 h post-exposure and then gradually decreased over a 1-week period (Figure 2f–j).[21] Instead, as shown in Figure 2k–o, most galectin-1 immunoreactivity in the CA3 subregion after kainate administration co-localized with glial fibrillary acidic protein (GFAP) immunoreactivity. From these results, we concluded that the systemic administration of kainate induces a gliotic response, namely the proliferation of astrocytes in the CA3 subregion. Thereafter, the activated astrocytes produce a large quantity of galectin-1.

To confirm that galectin-1 is indeed expressed in astrocytes, as seen in the hippocampus after kainate administration, we isolated astrocytes from neonatal mouse brains and examined their expression of galectin-1. As shown in Figure 3a (upper panel: cell extract), a substantial amount of galectin-1 was detected in the cultured astrocytes in the absence of kainate, and the level was increased more than two-fold 72 h after exposure to kainate (100 and 300 μM). Furthermore, we detected galectin-1 in conditioned media prepared from cultures of astrocytes in the presence or absence of kainate (Figure 3a, lower panel: medium). The amount of galectin-1 in the conditioned medium was slightly increased 24 h after the kainate exposure. The viability of astrocytes was not decreased in the presence of kainate and there was no detectable GAPDH (glyceraldehyde-3-phosphate dehydrogenase) protein in the conditioned media (data not shown). We therefore concluded that cultured astrocytes express and secrete galectin-1.

As shown in Figure 3b, immunofluorescence confocal microscopy revealed that galectin-1 was localized in the nucleus as well as in the cytoplasm of cultured astrocytes in the absence of kainate and its localization was not altered with kainate exposure (data not shown).

Galectin-1 deficiency does not affect the degeneration of CA3 pyramidal neurons or gliosis in the hippocampus induced by kainate administration. After kainate exposure, wild-type and galectin-1 knockout mice exhibited an almost identical time course as that of epileptiform seizure, and although the extent of the seizure was slightly lower in the galectin-1 knockout mice, this difference was not statistically significant (Figure 4a). Furthermore, the two groups of mice exhibited the same survival rate (100%) at 1 week after kainate administration. NeuN immunoreactivity in the CA3 subregion was not decreased in either wild-type or galectin-1 knockout mice (Figure 4b–e and j), indicating no apparent neuronal loss in the CA3 subregion. The mouse 129 strain used in this experiment is known to respond mildly to kainate as compared with other mouse strains,[22] and this may be the reason why we did not observe a loss of pyramidal cells in CA3. The extent of gliosis in the CA3 subregion was assessed by GFAP immunoreactivity, and we found that, after kainate administration, the GFAP index in

galectin-1 knockout mice was slightly lower than that in the wild-type mice; however, the difference between the two groups was not significant (Figure 4f–i and k). We thus concluded that the increased expression of galectin-1 in the hippocampus did not contribute to either the degeneration of the CA3 pyramidal neurons or to gliosis induced by the systemic administration of kainate.

Systemic administration of kainate also induces the expression of galectin-1 in the dentate gyrus and hippocampal hilus. Recently, it has been reported that galectin-1 is expressed in a subset of slowly dividing astrocytes in the subventricular zone (SVZ) of the lateral ventricle, including neural stem cells,[23] and it is also known that kainate-induced seizure is accompanied by enhanced neurogenesis in the subgranular zone (SGZ) of the dentate gyrus in the hippocampus.[5] We therefore hypothesized that the increased expression of galectin-1 after kainate administration may modulate the extent of neurogenesis in the dentate gyrus. To evaluate this hypothesis, we then examined the alteration of galectin-1 expression in this region, as well as the extent of proliferation of neural progenitors, after the systemic administration of kainate.

Mice were injected intraperitoneally with either saline (vehicle) or 30 mg/kg kainate and were then injected with 50 mg/kg 5-bromo-2′-deoxyuridine (BrdU) once a day for a week. The brain sections were examined under immunofluorescence confocal microscopy to detect BrdU, polysialylated neural cell adhesion molecule (PSA-NCAM) as a marker for young immature neurons,[3] and NeuN as a neural marker together with galectin-1 (Figure 5). In the untreated brains, the expression of galectin-1 was barely detectable in the dentate gyrus, whereas scattered cells with large soma in the hippocampal hilus exhibited a low but measurable level of galectin-1 expression (Figure 5b, j and r). After kainate administration, the expression level of galectin-1 was greatly increased, especially in the SGZ of the dentate gyrus (Figure 5f, n and v). The BrdU-positive population was significantly increased after kainate administration, as shown later in Figure 7, but most of BrdU-positive cells did not exhibit galectin-1 immunoreactivity (Figure 5e–h). However, it was noteworthy that we infrequently observed co-localization of galectin-1 immunoreactivity in a small population of BrdU-positive cells (Figure 5e–h; 5.53% arrowhead). PSA-NCAM-positive cells whose population was also significantly increased after kainate administration did not exhibit galectin-1 immunoreactivity (Figure 5m–p). Cells expressing doublecortin (DCX), another marker for young immature neurons,[3] were found in the SGZ after the exposure to kainate, and these

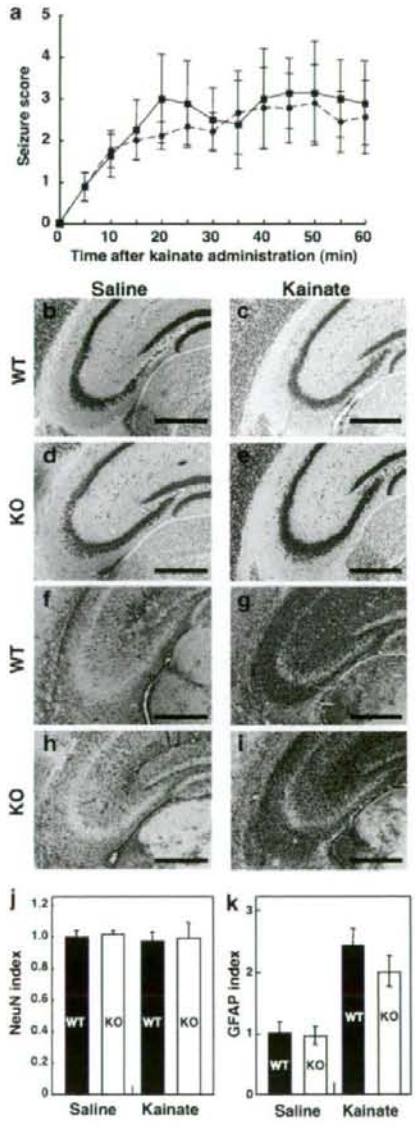

Figure 4 Galectin-1 deficiency does not affect kainate-induced degeneration of CA3 pyramidal cells or the proliferation of astrocytes in the hippocampus. (**a**) Seizure responses after kainate administration. Every 5 min for 1 h after kainate administration, the observed seizures were scored as described in Materials and Methods, and the mean ± SD value at each time point was plotted. Eight to nine mice per group were observed and scored. Square, wild-type mice; circle, galectin-1 knockout mice. (**b–e**) The mice were killed 1 week after kainate administration (kainate) or after saline injection (saline), and brain sections were prepared for NeuN immunohistochemistry. (f–i) Gliosis in the mouse hippocampus after kainate administration. Wild-type (WT) and galectin-1 knockout mice (KO) were injected with kainate (kainate) or saline (saline), and at 1 week after the injection, brains were removed and coronal sections were subjected to IHC with anti-GFAP antibody. (j) Galectin-1 deficiency does not affect neurodegeneration in the CA3 subregion after kainate administration. Each NeuN index relative to the value of the untreated group (saline) is shown as a bar graph with the mean ± SD (saline-injected mice, $N = 3$; kainate-injected mice, $N = 3$). There was no statistically significant difference between the wild-type (WT) and galectin-1 knockout mice (KO) (examined by the unpaired *t*-test). (**k**) Galectin-1 deficiency does not affect gliosis in the hippocampus after kainate administration. Each GFAP index relative to the value of the untreated group (saline) is shown as a bar graph with the mean ± SD (saline-injected mice, $N = 5$; kainate-injected mice, $N = 6$). There was no statistically significant difference between the wild-type (WT) and galectin-1 knockout mice (KO) (examined by the Mann–Whitney *U*-test). Scale bars = 500 μm

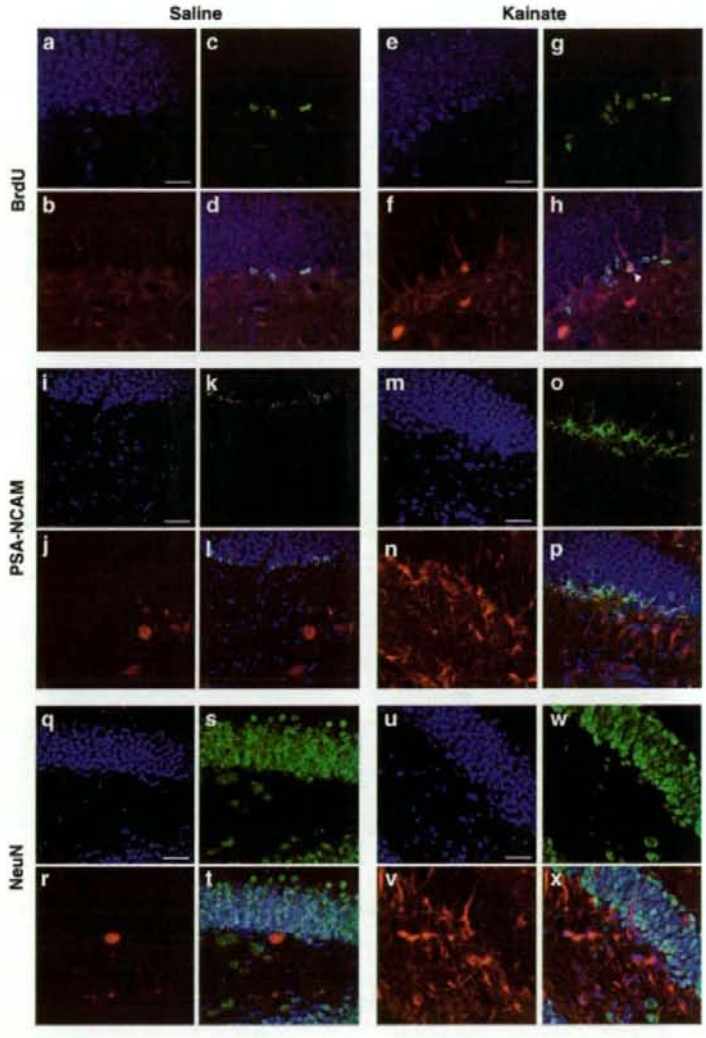

Figure 5 Kainate-induced cell proliferation in the dentate gyrus accompanied by the increased expression of galectin-1. After kainate administration (kainate), the mice were injected with BrdU once a day for 1 week, then brain sections were prepared and subjected to IHC. Untreated mice (saline) were injected with saline instead of kainate. (**a**–**h**) Cell proliferation and expression of galectin-1 in the dentate gyrus after kainate administration. DAPI (**a**, **e**; blue), galectin-1 (**b**, **f**; red), BrdU (**c**, **g**; green), and their merged images are shown (**d**, **h**). Out of 235 BrdU-positive cells, 13 cells (5.53%) exhibited galectin-1 immunoreactivity as shown by an arrowhead (**h**). (**i**–**p**) Distribution of newborn neurons and expression of galectin-1 in the dentate gyrus after kainate administration. DAPI (**i**, **m**; blue), galectin-1 (**j**, **n**; red), PSA-NCAM (**k**, **o**; green), and their merged images are shown (**l**, **p**). (**q**–**x**) Distribution of NeuN-positive cells and the expression of galectin-1 in the dentate gyrus after kainate administration. DAPI (**q**, **u**; blue), galectin-1 (**r**, **v**; red), NeuN (**s**, **w**; green), and their merged images are shown (**t**, **x**). Scale bars = 50 μm

were also mostly galectin-1-negative (Supplementary Figure S2). Furthermore, almost all NeuN-positive neurons were galectin-1-negative regardless of whether kainate was administered (Figure 5q–x).

To identify cells expressing galectin-1 in the dentate gyrus and hilus of the hippocampus, we next performed immunofluorescence confocal microscopy with antibodies against GFAP, S100β, or nestin together with the antibody against galectin-1 (Figure 6). GFAP-positive cells in the dentate gyrus and hilus of the hippocampus expressed an increased level of galectin-1 after the kainate exposure, as was seen in the CA3 subregion, and some of the galectin-1/GFAP double-positive cells in the SGZ extended their processes into the granular cell layer (GCL) (Figure 6a–h). On the other hand, S100β-positive astrocytes mostly distributed in the hilus also showed an increased expression of galectin-1 after the kainate exposure, and galectin-1-positive cells in the SGZ were mostly S100β-negative (Figure 6i–p). In addition, most

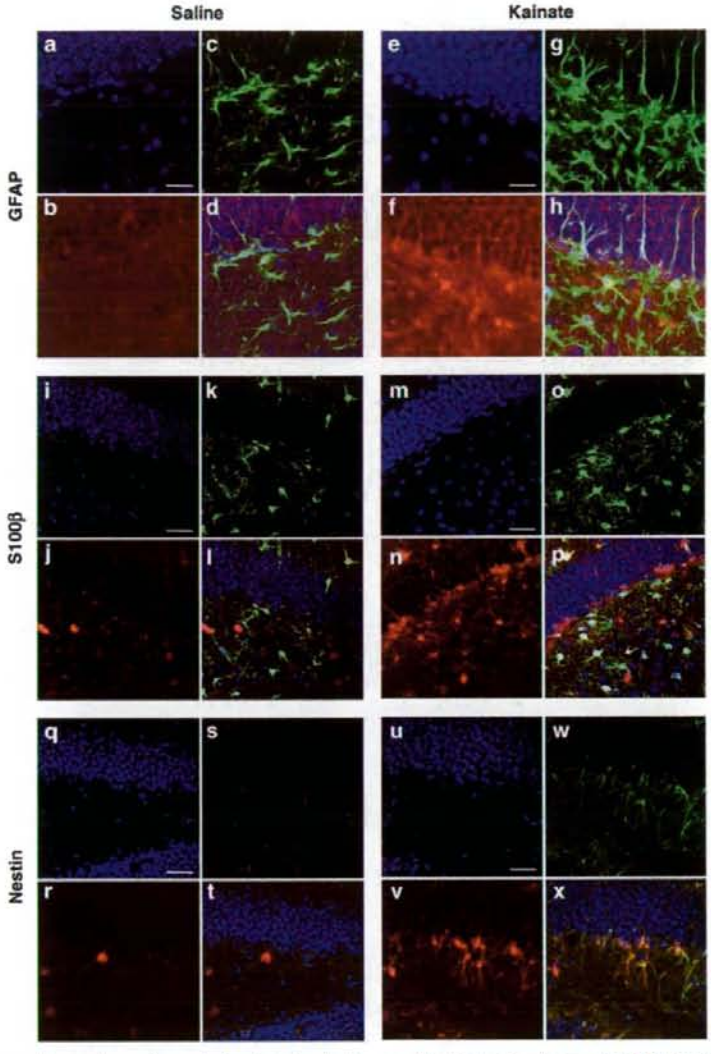

Figure 6 Galectin-1 is expressed in neural progenitors and astrocytes in the dentate gyrus after kainate-induced seizure. (**a–h**) Distribution of GFAP-positive cells and the expression of galectin-1 in the dentate gyrus after kainate administration. DAPI (**a**, **e**; blue), galectin-1 (**b**, **f**; red), GFAP (**c**, **g**; green), and their merged images are shown (**d**, **h**). (**i–p**) Distribution of S100β-positive cells and expression of galectin-1 in the dentate gyrus after kainate administration. DAPI (**i**, **m**; blue), galectin-1 (**j**, **n**; red), S100β (**k**, **o**; green), and their merged images are shown (**l**, **p**). (**q–x**) Distribution of nestin-positive cells and the expression of galectin-1 in the dentate gyrus after kainate administration. DAPI (**q**, **u**; blue), galectin-1 (**r**, **v**; red), nestin (**s**, **w**; green), and their merged images are shown (**t**, **w**). Scale bars = 50 μm

nestin-positive cells representing neural progenitors in the SGZ,[3] which appeared after the kainate exposure, were found to express galectin-1 (Figure 6q–x).

Galectin-1 deficiency attenuates both of basal and of kainate-induced proliferation of neural progenitors in the adult mouse hippocampus. In order to clarify the role of galectin-1 in kainate-induced neurogenesis in the dentate gyrus, we compared numbers of BurU-positive cells in the dentate GCL of wild-type and galectin-1 knockout mice administered saline or kainate. Counts were obtained using unbiased stereological counting techniques. In control groups administered saline, the density of BrdU-positive cells in the GCL of galectin-1 knockout mice (mean $\pm$ SD = 7560 $\pm$ 825 cells per mm^3) was 62% of that seen in the wild-type mice (12 222 $\pm$ 2833 cells per mm^3) ($P < 0.05$) (Figure 7a, b and e). Furthermore, the numbers of BrdU-positive cells in the GCL of both wild-type and galectin-1 knockout mice were remarkably increased 1 week after kainate administration (Figure 7c and d), and the density of these cells in the GCL of galectin-1 knockout mice (19 185 $\pm$ 5624 cells per mm^2) was again 52% of that seen

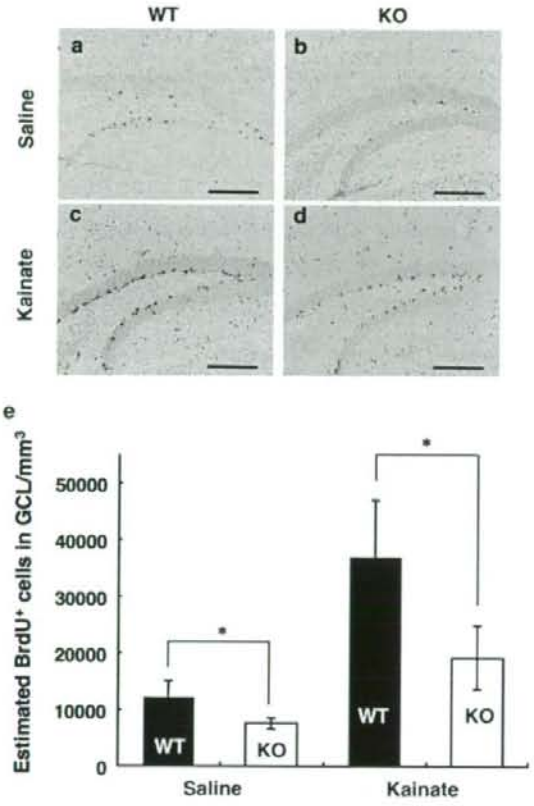

Figure 7 Galectin-1 deficiency attenuates both of basal and kainate-induced proliferation of neural progenitors in the dentate gyrus. After kainate administration (kainate), the mice were injected with BrdU once a day for 1 week, then brain sections were prepared and subjected to IHC to detect BrdU-positive cells. Untreated mice (saline) were injected with saline instead of kainate. (**a–d**) Detection of BrdU-positive cells in the mouse hippocampus with or without kainate administration. (**e**) Galectin-1 knockout mice exhibited a significant reduction in the number of BrdU-positive cells in the hippocampal GCL with or without kainate administration. Brain sections from each group ($N=5$) were prepared and subjected to IHC to detect BrdU-positive cells in this region. The density of BrdU-positive cells in the hippocampal GCL was determined stereologically (cells per mm^3), and is shown in the bar graph with the mean ± SD. Black bar, wild-type mice; white bar, galectin-1 knockout mice. Mann–Whitney *U*-test, $^*P<0.05$. Scale bars = 500 μm

in wild-type mice (36 952 ± 9979 cells per mm^2) ($P<0.05$) (Figure 7e). In galectin-1 knockout mice, the kainate-induced increase in the density of BrdU-positive cells (mean increase = 11 625 cells per mm^3) was about 47% of that seen in the wild-type mice (mean increase = 24 730 cells per mm^3). There was no significant difference in the volume of the dentate GCL between the two mouse strains with or without kainate administration (data not shown).

We finally performed immunofluorescence confocal microscopy to confirm that the BrdU-positive cells in the dentate SGZ express DCX or NeuN (Supplementary Figure S3), and found that more than 70% of the BrdU-positive cells were DCX-positive both in wild-type and galectin-1 knockout mice regardless of kainate administration. Furthermore, 70–80% of the BrdU-positive cells were also NeuN-positive both in wild-type and in galectin-1 knockout mice. About half of DCX-positive cells in the SGZ express lower levels of NeuN in comparison to NeuN-positive neurons in GCL (Supplementary Figure S4), indicating that they are young immature neurons. We thus concluded that galectin-1 deficiency significantly attenuates proliferation of neural progenitors in the dentate gyrus of the adult mouse hippocampus both in the presence and absence of brain insult.

Discussion

In this study, we found for the first time that the expression of the galectin-1 gene, both at mRNA and protein levels, is highly induced in activated astrocytes in the CA3 subregion and the dentate gyrus of the adult mouse hippocampus after epileptic seizure caused by the systemic administration of kainate. Furthermore, we showed that galectin-1 deficiency results in attenuated proliferation of neural progenitors in the dentate gyrus both in the presence and absence of brain insult, showing that galectin-1 enhances proliferation of neural progenitors in the adult mouse hippocampus.

Recently, Sakaguchi *et al.*[23] reported that neural stem cells in the SVZ express galectin-1, and that the population of BrdU-positive cells in the SVZ of galectin-1 knockout mice was 50% of that seen in the wild-type mice. Furthermore, they showed that recombinant galectin-1 promoted the proliferation of neural stem cells both *in vitro* and *in vivo*. In this study, we found that a substantial level of galectin-1 is expressed in the hippocampus of normal mice (Figure 1), and that the density of BrdU-positive cells in the dentate GCL of galectin-1 knockout mice was 62% of that seen in the wild-type mice (Figure 7). As more than 70% of BrdU-positive cells in the GCL of both mouse strains were either DCX- or NeuN-positive, markers for newborn neurons or neural cells, respectively[3] (Supplementary Figure S3), our results indicate that galectin-1 may promote basal neurogenesis in the GCL as well as in the SVZ under normal conditions.

The level of galectin-1 mRNA in the hippocampus began to increase within 1 day of kainate administration and reached a peak within 3 days, followed by an increased expression of galectin-1 protein in the CA3 subregion and the dentate gyrus of the hippocampus 1 week after the exposure (Figure 1). Immunofluorescence confocal microscopy revealed that activated astrocytes in the CA3 subregion and the dentate gyrus as well as neural progenitors in the SGZ of the dentate gyrus had a significantly increased expression of galectin-1 after exposure to kainate (Figures 2 and 6). We isolated astrocytes from neonatal mouse brains, and showed that astrocytes do indeed express and secrete galectin-1 in culture, and that this expression was increased in the presence of kainate (Figure 3). Adult neurogenesis in either the SGZ or SVZ is reported to be enhanced after insult to the brain.[5,13,24–26] After kainate was administered to wild-type mice, the density of BrdU-positive cells in the GCL increase significantly (mean increase = 24 730 cells per mm^3); however, after it was administered to galectin-1 knockout mice, a lower increase in the density (mean increase = 11 625 cells per mm^3) was observed. Again, more than 70% of

BrdU-positive cells in both mouse strains were either DCX- or NeuN-positive, indicating that galectin-1 also promotes insult-induced proliferation of neural progenitors in the dentate gyrus. We thus concluded that galectin-1 expressed in activated astrocytes may be involved in the promotion of insult-induced neurogenesis in the dentate gyrus. Recently, it has been reported that a lack of galectin-1 results in defects in myoblast fusion and muscle regeneration after cardiotoxin injury.[27] Taken together, we may suggest that galectin-1 plays an important role during tissue regeneration in response to insults in general.

It is known that astrocytes promote neurogenesis in the adult hippocampus,[28] and we showed in this study that when the hippocampus underwent kainate-induced seizure, activated astrocytes predominantly expressed galectin-1 not only in the CA3 subregion but also in the dentate gyrus, where seizure-induced neurogenesis takes place. Furthermore, in the dentate gyrus, galectin-1 is expressed in GFAP- or nestin-positive but PSA-NCAM/NeuN/BrdU-negative cells, which are likely to be slowly dividing neural progenitors.[3,29,30] As shown in Figure 5e–h, we infrequently observed co-localization of galectin-1 immunoreactivity in a small population of BrdU-positive cells after kainate administration, which may represent the slowly dividing neural progenitors. Taken together, we propose that, after kainate-induced seizure, activated astrocytes and neural progenitors produce and secrete galectin-1 and that the secreted galectin-1 promotes proliferation or survival of the latter cells, thus enhancing neurogenesis in the dentate gyrus (Figure 8).

It is most likely that the galectin-1 secreted from the activated astrocytes functions as a growth-stimulating or survival factor for neural stem cells or progenitors as astrocytes are known to constitute a niche for these types of cells. Galectin-1 is a multifunctional molecule, but the mechanisms for how galectin-1 functions in the central nervous system are not yet well known. It has been reported that galectin-1 induces brain derived neurotrophic factor (BDNF) in astrocytes.[31] Furthermore, it was also reported that BDNF promotes adult neurogenesis.[3,32] Astrocytes expressing galectin-1 may thus increase the supply of such neurotrophic factors to promote neurogenesis after brain insults.

Axonal regeneration after axotomy of the peripheral nerves is known to be significantly promoted by an oxidized monomeric form of galectin-1 but not by the natural dimeric form.[20,33] It has been shown that oxidized galectin-1 acts directly on macrophages, which in turn may produce a factor that promotes axonal growth.[33] We have shown earlier that exposure to kainate significantly increases oxidative stress in the hippocampus and that oxidative damage of cellular components is accumulated in hippocampal neurons, astrocytes, and microglias.[21] Therefore, we suggest that astrocyte-secreted galectin-1, which is likely to be mostly oxidized, may function in promoting neurogenesis in the dentate gyrus. Identification of the receptor(s) and interacting molecules on these cells would shed light on the network used to regulate insult-induced neurogenesis.

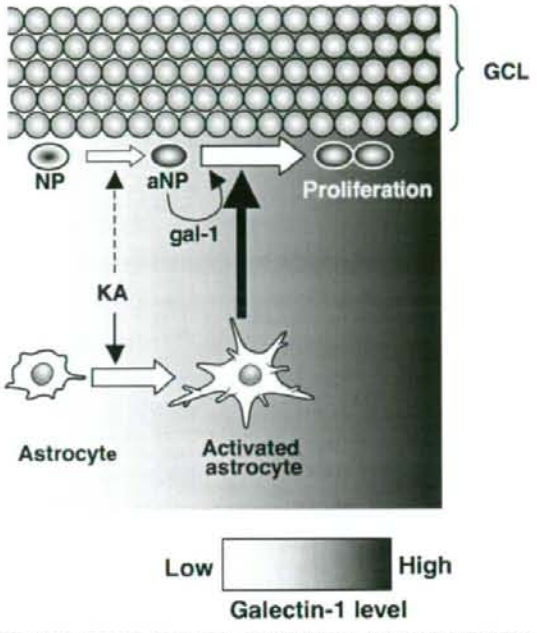

Figure 8 The role of galectin-1 in insult-induced neurogenesis in the dentate gyrus. Kainate administration activates astrocytes and neural progenitors, which results in an increased secretion of galectin-1 in the hippocampal formation. The secreted galectin-1 promotes the proliferation or survival of neural progenitors in the SGZ of dentate gyrus, thereby promoting neurogenesis. The gradient shown at the bottom indicates the level of galectin-1 protein in the niche. Gal-1, galectin-1; KA, kainate; NP, neural progenitor; aNP, activated neural progenitor; GCL, granule cell layer

Materials and Methods

Antibodies. Mouse monoclonal antibody to BrdU (BMC9318, 1 : 800) was obtained from Roche Diagnostics Japan (Tokyo, Japan). Rat monoclonal antibody to BrdU (BU1/75 (ICR1) 1 : 1000) was obtained from Abcam KK (Tokyo, Japan). The rabbit polyclonal antibodies (anti-rhGal-1) against recombinant human galectin-1 have been described earlier.[20] Mouse monoclonal antibody to GFAP (G-A-5, 1 : 15 000), a marker for astrocytes, and mouse monoclonal antibody to S100*β* (SH-B1, 1 : 1000), which is a specific marker for astrocytes, were purchased from Sigma-Aldrich Japan KK (Tokyo, Japan). Rat monoclonal antibody to F4/80 (Cl:A3-1, 1 : 500), a marker for microglia, was purchased from SEROTEC (Oxford, UK). Mouse monoclonal antibody to NeuN (A60, 1 : 30 000), a marker for mature neurons, and mouse monoclonal antibody to PSA-NCAM (2-2B, 1 : 800) were purchased from Chemicon (Temecula, CA, USA). Mouse monoclonal antibody to nestin (rat401, 1 : 400) was purchased from BD Bioscience Pharmingen (San Jose, CA, USA). Goat polyclonal antibody to DCX was purchased from Santa Cruz Technology (Santa Cruz, CA, USA). Alexa Fluor-labeled second antibodies were obtained from Invitrogen Japan (Tokyo, Japan).

Animals. For the analysis of galectin-1 expression by IHC, RT-PCR and western blotting, we used C57BL/6J mice (Clea Japan Inc., Tokyo, Japan). Galectin-1 knockout (129 P3/J *Lgals1*$^{-/-}$) and wild-type mice (129 P3/J *Lgals1*$^{+/+}$), described earlier,[34] were used to compare seizure responses, gliosis, and neurogenesis after kainate administration. All animals were maintained in an air-conditioned specific pathogen-free room with a time-controlled lighting system. The handling and killing of all animals were carried out in accordance with nationally prescribed guidelines, and ethical approval for the study was granted by the Animal Care and Use Committee (Kyushu University, Fukuoka, Japan).

Experimental design and kainate treatment. Eight- to 10-week-old male mice were used for this study. The mice were injected intraperitoneally with either saline (vehicle) or 30 mg/kg kainate (Wako, Osaka, Japan) dissolved in saline.

and were then injected daily for 1 week with 50 mg/kg BrdU (Sigma-Aldrich Japan KK, Tokyo, Japan) dissolved in saline. To compare the degree of epileptiform seizure, we observed mice for 1 h after kainate administration and recorded the seizure score: 0, no reaction; 1, arrest of motion; 2, myoclonic jerks of the head and neck, with brief twitching movements; 3, unilateral clonic activity; 4, bilateral forelimb tonic and clonic activity; and 5, generalized tonic-clonic activity with loss of postural tone as well as death from continuous convulsion, according to previously described criteria.[21,35] Animals were killed 1 day after the last BrdU injection, unless otherwise noted.

Tissue processing and IHC. The animals were deeply anesthetized with pentobarbital (30 mg/kg, i.p.) and were perfused intracardially with saline followed by cold 4% paraformaldehyde in 0.1 M PBS. The brains were removed, immersed for 12 h in the same 4% paraformaldehyde fixative at 4 °C, and cryoprotected in 20 and 30% sucrose in PBS for 48 h at 4 °C. The brains were then frozen and stored at −80 °C until use. Serial coronal sections (40 μm thickness) were cut on a cryostat, collected as free-floating sections (40 μm thickness) in PBS, and then were processed immediately for IHC, according to previously described methods.[21] Digital images were acquired using Axioskop2 Plus equipped with a CCD camera, AxioCam (Carl Zeiss MicroImaging Japan, Tokyo, Japan).

Quantitative analysis of galectin-1 and NeuN expression in the hippocampus. Galectin-1 and NeuN immunostaining was performed with four representative coronal sections from each brain sample. All acquired digital images were processed uniformly at a threshold in gray-scale mode to subtract any background corresponding to areas without tissue, using Adobe Photoshop version 7.0 (Adobe Systems, San Jose, CA, USA). The intensity of each immunoreactivity in a given area of hippocampus (CA3 subregion) was measured using Image Gauge version 3.2 (Fujifilm, Tokyo, Japan). Representative coronal sections were measured and the mean intensity of each immunoreactivity was calculated for each animal as the galectin-1 or NeuN index in CA3.

Quantitative analysis of gliosis by immunohistochemical detection. GFAP immunostaining was performed with six coronal sections from each brain sample corresponding to each first section of six serial sections (bregma −2.54 to −1.70 mm).[36] All acquired digital images were processed uniformly at a threshold in gray-scale mode to subtract any background corresponding to the area without tissue, using Adobe Photoshop version 7.0. The intensity of GFAP immunoreactivity in any given area of the CA3 subregions was measured using Image Gauge version 3.2. Six representative coronal sections with two hippocampus formations corresponding to each first section of six serial sections (bregma −2.54 to −1.70 mm) were measured and the mean intensity of GFAP immunoreactivity was calculated as the GFAP index for each individual animal.

Counting BrdU-positive cells using unbiased stereological counting techniques. Free-floating sections were incubated in 70% formamide in 2 × SSC for 2 h at 65 °C. The sections were washed in PBD (Triton X-100, 0.3% in PBS) and immersed in H_2O for 10 min. In addition, the sections were treated with 2 N HCl at room temperature for 30 min, thereby denaturing the nuclear DNA, and were then treated with Tris-HCl (pH 7.5) for 10 min and subjected to IHC with the anti-BrdU antibody. The numbers of BrdU-positive cells in the dentate GCL and in corresponding sample volumes were determined in nine coronal sections, 120 μm apart (bregma −2.46 to −1.34 mm),[36] using a semiautomatic stereology system (StereoInvestigator, MBF Bioscience, Williston, VT, USA). Cells that met the counting criteria through a 40-μm axial distance were counted according to the optical dissector principle.[37] The GCL reference volume was determined by summing the traced granule cell area for each section multiplied by the distance between sections sampled.

Immunofluorescence confocal microscopy. Free-floating sections incubated with an appropriate primary antibody were then incubated with an Alexa Fluor-labeled second antibody for 45 min at room temperature. The sections were further incubated in a solution containing 0.05 μg/ml DAPI (Sigma-Aldrich Japan KK) for 10 min at room temperature, and mounted on slides with Vectashield (Vector Laboratories, Burlingame, CA, USA). Confocal images were acquired using Eclipse TE300 (Nikon, Kanagawa, Japan) equipped with the Radiance 2100 laser-scanning confocal microscope system (Bio-Rad Laboratories, Hercules, CA, USA) or an LSM510 META Confocal Microscope System (Carl Zeiss MicroImaging Japan). All sections from each experimental animal and the groups to be compared were processed in parallel.

Real-time RT-PCR analysis. Total RNA from the hippocampus of C57BL/6J mice was prepared using ISOGEN (Nippongene, Tokyo, Japan), and the obtained RNA was treated with RNase-free DNase, according to the manufacturer's instructions. RT-PCR for galectin-1 and GAPDH mRNAs was performed as follows. First-strand cDNA, which was synthesized using a High Capacity cDNA Reverse Transcription Kit (Applied Biosystems Japan, Tokyo, Japan) according to the manufacturer's instructions, was subjected to real-time PCR. RT-PCR and the detection of the PCR product in real time were performed using with a POWER SYBR® GREEN PCR MASTER MIX and an ABI PRISM 7000 Sequence Detection System (Applied Biosystems Japan). Serially diluted cDNA was used to obtain a standard curve for each transcript. Primers for galectin-1 mRNA (gal1-F: CCTGGTCCATCTTCACTTCCAT; gal1-R: CTTTGGCCTGGAAAGCACAA) were obtained from Sigma-Aldrich Japan KK, and those for GAPDH mRNA (gapdh-F: AAATGGTGAAGGTCGGTGTG; gapdh-R: TGAAGGGGTCGTTGATGG) were obtained from TAKARA BIO (Shiga, Japan).

Western blotting. Mouse hippocampi were homogenized on ice in 200–400 μl of lysis buffer containing 50 mM Tris-HCl, pH 8.0, 150 mM NaCl, 0.5% sodium deoxycholate, 1% NP40, 0.1% SDS, and protease inhibitor cocktail (Nacalai Tesque, Kyoto, Japan) using a Potter-type homogenizer. The lysates were centrifuged at 100 000 × *g* for 30 min and then the supernatants were recovered. Hippocampal lysates were subjected to SDS-PAGE (15%) followed by western blotting using anti-rhGal-1 (500 ng/ml), according to a previously described method.[38] Recombinant mouse galectin-1 (rmGal-1) expressed in *Escherichia coli* BL21 cells carrying pET8c: rmGal-1 was used as a standard.[14] The amount of protein was measured using Image Gauge version 3.2.

Astrocyte culture. Primary astrocytes were prepared from the cerebral cortex of 1-day-old C57BL/6J mice, according to a method described earlier.[39] Isolated astrocytes were maintained for 2 weeks in Dulbecco's modified Eagle's medium (Nissui, Tokyo, Japan) containing 10% fetal calf serum (Hyclone, Logan, UT, USA), 0.5 μg/ml insulin (Nacalai Tesque, Kyoto, Japan), 2 mM L-glutamine, 100 U/ml penicillin, 100 mg/ml streptomycin, and 0.2% $NaHCO_3$ at 37 °C in 10% CO_2/90% air. The cell composition of the cultures was checked by immunostaining for S100β, NeuN, and Iba-1. Cultures containing more than 95–99% S100β-positive cells were used (data not shown). Seeded astrocytes were kept in the serum-free medium with or without kainate for up to 2 days. After exposure to kainate, conditioned medium and astrocytes were collected and subjected to western blotting using anti-rhGal-1 (500 ng/ml), according to a previously described method.[38] The conditioned medium was precipitated with trichloroacetic acid before western blotting.

Statistical analysis. The data are expressed as mean ± SD. Relative IR comparison, western blotting analysis, real-time RT-PCR data, and NeuN index were compared using an unpaired *t*-test, and other data were compared using the Mann–Whitney *U*-test. A level of $P < 0.05$ was considered statistically significant.

Acknowledgements. We are grateful to Dr. Kanba for providing us with the opportunity to conduct this study, and Dr. W Campbell for useful comments on this manuscript. We thank S Kitamura and A Matsuyama for their technical expertise. This work was supported by grants from the Ministry of Education, Culture, Sports, Science, and Technology of Japan and the Japan Society for the Promotion of Science (to Y Nakabeppu); the 21st Century Centers of Excellence Program of MEXT (to Kyushu University); Kyushu University Interdisciplinary Programs in Education and Projects in Research Development (to K Kajitani); and Ligue Contre le Cancer, Comite de Paris, and Association Contre le Cancer (to F Poirier).

1. Morrison JH, Hof PR. Life and death of neurons in the aging brain. *Science* 1997; **278**: 412–419.
2. Meltzer LA, Yabaluri R, Deisseroth K. A role for circuit homeostasis in adult neurogenesis. *Trends Neurosci* 2005; **28**: 653–660.
3. Zhao C, Deng W, Gage FH. Mechanisms and functional implications of adult neurogenesis. *Cell* 2008; **132**: 645–660.
4. Liu J, Solway K, Messing RO, Sharp FR. Increased neurogenesis in the dentate gyrus after transient global ischemia in gerbils. *J Neurosci* 1998; **18**: 7768–7778.

5. Gray WP, Sundstrom LE. Kainic acid increases the proliferation of granule cell progenitors in the dentate gyrus of the adult rat. *Brain Res* 1998; **790**: 52–59.
6. Herdegen T, Leah JD. Inducible and constitutive transcription factors in the mammalian nervous system: control of gene expression by Jun, Fos and Krox, and CREB/ATF proteins. *Brain Res Brain Res Rev* 1998; **28**: 370–490.
7. Nakabeppu Y, Ryder K, Nathans D. DNA binding activities of three murine Jun proteins: stimulation by Fos. *Cell* 1988; **55**: 907–915.
8. Nakabeppu Y, Nathans D. A naturally occurring truncated form of FosB that inhibits Fos/Jun transcriptional activity. *Cell* 1991; **64**: 751–759.
9. Nakabeppu Y, Oda S, Sekiguchi M. Proliferative activation of quiescent Rat-1A cells by ΔFosB. *Mol Cell Biol* 1993; **13**: 4157–4166.
10. Oda S, Nishida J, Nakabeppu Y, Sekiguchi M. Stabilization of cyclin E and cdk2 mRNAs at G1/S transition in Rat-1A cells emerging from the G0 state. *Oncogene* 1995; **10**: 1343–1351.
11. Nishioka T, Sakumi K, Miura T, Tahara K, Horie H, Kadoya T *et al.* FosB gene products trigger cell proliferation and morphological alteration with an increased expression of a novel processed form of galectin-1 in the rat 3Y1 embryo cell line. *J Biochem* 2002; **131**: 653–661.
12. Tahara K, Tsuchimoto D, Tominaga Y, Asoh S, Ohta S, Kitagawa M *et al.* FosB, but not FosB, induces delayed apoptosis independent of cell proliferation in the Rat1a embryo cell line. *Cell Death Differ* 2003; **10**: 496–507.
13. Kurushima H, Ohno M, Miura T, Nakamura TY, Horie H, Kadoya T *et al.* Selective induction of ΔFosB in the brain after transient forebrain ischemia accompanied by an increased expression of galectin-1, and the implication of ΔFosB and galectin-1 in neuroprotection and neurogenesis. *Cell Death Differ* 2005; **12**: 1078–1096.
14. Miura T, Takahashi M, Horie H, Kurushima H, Tsuchimoto D, Sakumi K *et al.* Galectin-1beta, a natural monomeric form of galectin-1 lacking its six amino-terminal residues promotes axonal regeneration but not cell death. *Cell Death Differ* 2004; **11**: 1076–1083.
15. Miura T, Ohnishi Y, Kurushima H, Horie H, Kadoya T, Nakabeppu Y. Regulation of the neuronal fate by DeltaFosB and its downstream target, galectin-1. *Curr Drug Targets* 2005; **6**: 437–444.
16. Barondes SH, Cooper DN, Gitt MA, Leffler H. Galectins. Structure and function of a large family of animal lectins. *J Biol Chem* 1994; **269**: 20807–20810.
17. Hsu DK, Liu FT. Regulation of cellular homeostasis by galectins. *Glycoconj J* 2004; **19**: 507–515.
18. Scott K, Weinberg C. Galectin-1: a bifunctional regulator of cellular proliferation. *Glycoconj J* 2004; **19**: 467–477.
19. Puche AC, Poirier F, Hair M, Bartlett PF, Key B. Role of galectin-1 in the developing mouse olfactory system. *Dev Biol* 1996; **179**: 274–287.
20. Horie H, Inagaki Y, Sohma Y, Nozawa R, Okawa K, Hasegawa M *et al.* Galectin-1 regulates initial axonal growth in peripheral nerves after axotomy. *J Neurosci* 1999; **19**: 9964–9974.
21. Kajitani K, Yamaguchi H, Dan Y, Furuichi M, Kang D, Nakabeppu Y. MTH1, an oxidized purine nucleoside triphosphatase, suppresses the accumulation of oxidative damage of nucleic acids in the hippocampal microglia during kainate-induced excitotoxicity. *J Neurosci* 2006; **26**: 1688–1698.
22. Royle SJ, Collins FC, Rupniak HT, Barnes JC, Anderson R. Behavioural analysis and susceptibility to CNS injury of four inbred strains of mice. *Brain Res* 1999; **816**: 337–349.
23. Sakaguchi M, Shingo T, Shimazaki T, Okano HJ, Shiwa M, Ishibashi S *et al.* A carbohydrate-binding protein, galectin-1, promotes proliferation of adult neural stem cells. *Proc Natl Acad Sci USA* 2006; **103**: 7112–7117.
24. Parent JM, Yu TW, Leibowitz RT, Geschwind DH, Sloviter RS, Lowenstein DH. Dentate granule cell neurogenesis is increased by seizures and contributes to aberrant network reorganization in the adult rat hippocampus. *J Neurosci* 1997; **17**: 3727–3738.
25. Jin K, Minami M, Lan JQ, Mao XO, Batteur S, Simon RP *et al.* Neurogenesis in dentate subgranular zone and rostral subventricular zone after focal cerebral ischemia in the rat. *Proc Natl Acad Sci USA* 2001; **98**: 4710–4715.
26. Jin K, Galvan V, Xie L, Mao XO, Gorostiza OF, Bredesen DE *et al.* Enhanced neurogenesis in Alzheimer's disease transgenic (PDGF-APP$_{Sw,Ind}$) mice. *Proc Natl Acad Sci USA* 2004; **101**: 13363–13367.
27. Georgiadis V, Stewart HJ, Pollard HJ, Tavsanoglu Y, Prasad R, Horwood J *et al.* Lack of galectin-1 results in defects in myoblast fusion and muscle regeneration. *Dev Dyn* 2007; **236**: 1014–1024.
28. Song H, Stevens CF, Gage FH. Astroglia induce neurogenesis from adult neural stem cells. *Nature* 2002; **417**: 39–44.
29. Kempermann G, Jessberger S, Steiner B, Kronenberg G. Milestones of neuronal development in the adult hippocampus. *Trends Neurosci* 2004; **27**: 447–452.
30. Sakaguchi M, Imaizumi Y, Okano H. Expression and function of galectin-1 in adult neural stem cells. *Cell Mol Life Sci* 2007; **64**: 1254–1258.
31. Sasaki T, Hirabayashi J, Manya H, Kasai K, Endo T. Galectin-1 induces astrocyte differentiation, which leads to production of brain-derived neurotrophic factor. *Glycobiology* 2004; **14**: 357–363.
32. Lee J, Duan W, Mattson MP. Evidence that brain-derived neurotrophic factor is required for basal neurogenesis and mediates, in part, the enhancement of neurogenesis by dietary restriction in the hippocampus of adult mice. *J Neurochem* 2002; **82**: 1367–1375.
33. Horie H, Kadoya T, Hikawa N, Sango K, Inoue H, Takeshita K *et al.* Oxidized galectin-1 stimulates macrophages to promote axonal regeneration in peripheral nerves after axotomy. *J Neurosci* 2004; **24**: 1873–1880.
34. Poirier F, Robertson EJ. Normal development of mice carrying a null mutation in the gene encoding the L14 S-type lectin. *Development* 1993; **119**: 1229–1236.
35. Yang DD, Kuan CY, Whitmarsh AJ, Rincon M, Zheng TS, Davis RJ *et al.* Absence of excitotoxicity-induced apoptosis in the hippocampus of mice lacking the *Jnk3* gene. *Nature* 1997; **389**: 865–870.
36. Franklin KB, Paxinos G. *The Mouse Brain in Stereotaxic Coordinates*. Academic Press: New York, 2001.
37. Kempermann G, Kuhn HG, Gage FH. Experience-induced neurogenesis in the senescent dentate gyrus. *J Neurosci* 1998; **18**: 3206–3212.
38. Tsuchimoto D, Sakai Y, Sakumi K, Nishioka K, Sasaki M, Fujiwara T *et al.* Human APE2 protein is mostly localized in the nuclei and to some extent in the mitochondria, while nuclear APE2 is partly associated with proliferating cell nuclear antigen. *Nucleic Acids Res* 2001; **29**: 2349–2360.
39. Lyons SA, Kettenmann H. Oligodendrocytes and microglia are selectively vulnerable to combined hypoxia and hypoglycemia injury *in vitro*. *J Cereb Blood Flow Metab* 1998; **18**: 521–530.

Supplementary Information accompanies the paper on Cell Death and Differentiation website (http://www.nature.com/cdd)

Legends to Supplementary Figures

Supplementary Figure S1 Specific detection of galectin-1 in wild-type but not galectin-1 knockout mice by anti-rhGal-1. In order to demonstrate the specificity of anti-rhGal-1, sections from wild-type and galectin-1 knockout (KO) mice were subjected to immunohistochemical detection using the anti-rhGal-1. (a) In an untreated wild-type mouse, expression of galectin-1 was detected in the hippocampus. (b) One week after kainate administration, the population of galectin-1-positive cells was significantly increased in hippocampus. (c, d) No immunoreactive signal was detected in galectin-1 knockout mice regardless of kainate administration. Scale bars: 200 μm.

Supplementary Figure S2 Doublecortin-positive newborn neurons in dentate gyrus were galectin-1 negative. Brain sections from wild-type mice 7 days after saline (a-d) or kainate administration (e-f) were subjected to immunofluorescence confocal microscopy using the anti-rhGal-1 and anti-doublecortin. DAPI (a, e; blue), galectin-1 (b, f; red), doublecortin (c, g; green), and their merged images are shown (d, h). Scale bars: 50 μm.

Supplementary Figure S3 BrdU-positive cells express neural markers both in galectin-1 knockout and wild-type mice a week after kainate administration. In order to characterize the property of BrdU-positive cells, we performed immunofluorescence confocal microscopy for DCX/BrdU and NenN/BrdU, with 3 representative coronal sections from each mouse (N=3). (a-l) BrdU-positive cells express a young immature neuron marker, doublecortin (DCX). DCX (a, d, g, j; green), BrdU (b, e, h, k; red), and their merged images are shown (c, f, i, l). D^+/B^+ indicates the ratio of DCX-positive cells to BrdU-positive cells expressed as a percentage. (m-x) BrdU-positive cells express a neural marker, NeuN. NeuN (m, p, s, v; green), BrdU (n, q, t, w; red), and their merged images are shown (o, r, u, x). N^+/B^+ indicates the ratio of NeuN-positive cells to BrdU-positive cells expressed as a percentage. Scale bars: 25 μm.

Supplementary Figure S4 Many DCX-positive cells are NeuN-positive, indicating a temporal overlap between the two markers a week after kainate administration. In order to characterize the property of DCX-positive cells, we performed immunofluorescence confocal microscopy for DCX/NeuN with representative coronal sections from wild-type mice. One week after kainate administration, DCX-positive cells exhibit lower levels of NeuN immuoreactivity in comparison to NeuN-positive neurons in GCL. DCX (a; green), NeuN (b, red), and their merged image is shown (c). Scale bar: 25 μm.